Neotectonics of Arc-Continent Collision
Manizales, Colombia

Field Trip Guide

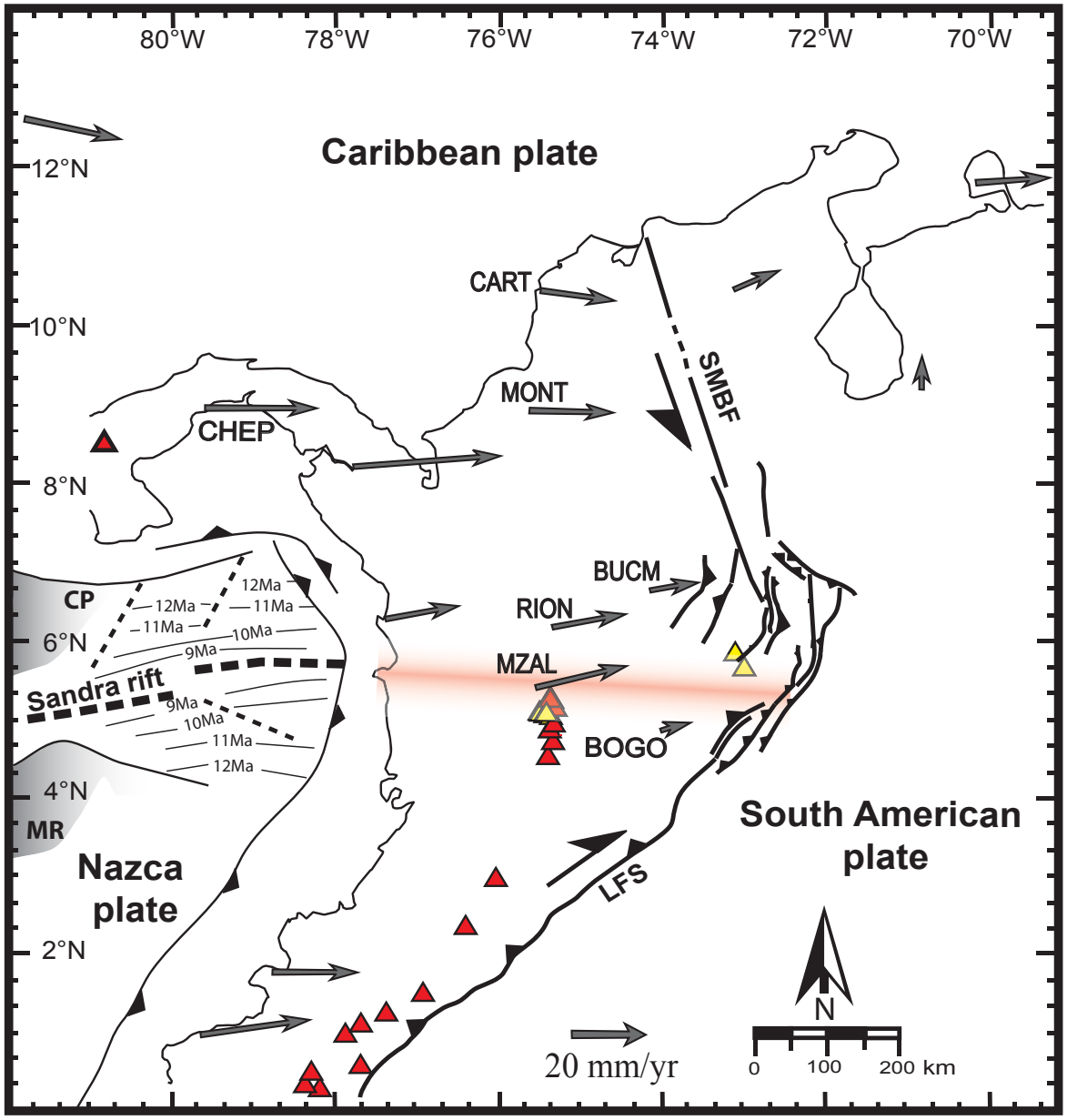

17-21 January, 2011

A GSA Penrose Meeting

By Carlos Borrero, Alvaro Nivia, Carlos Vargas and Paul Mann

The Geological Society of America, Penrose Meeting:
Neotectonics of arc-continent collision
Manizales, Colombia, January 17-21, 2011

Field guides for day excursions to the Nevado del Ruiz volcano on Tuesday, January 18, and to the Romeral fault system on Thursday, January 20, 2011

Part 1: Map showing routes for both field trips and general field trip information

Part 2: Tectonic setting of the field trip areas from sedimentary basins to subducted slabs in the upper mantle (Discussion leaders: Carlos A. Vargas and Paul Mann)

Part 3: Field guide to the tectonic setting and stratigraphy of the Nevado del Ruiz volcano (Field trip leader: Carlos Borrero, with assistance from Maria Luisa Monsalve and Carlos A. Vargas)

Part 4: Field guide to the Romeral fault system, Colombia: A suture zone between continental and accreted oceanic crust (Field trip leader: Alvaro Nivia, with assistance from Fabio Cediel, Andreas Kammer, Hector Mora, Hans Diederix, and Carlos A. Vargas)

Part 1: Map showing routes for both field trips and general field trip information

Figure 1 shows the regional setting of Colombia, the southwestern Caribbean and the eastern Pacific Ocean. Manizales is located in the western Cordillera of Colombia near the Ncvado del Ruiz volcano. Manizales is the capital of the Department of Caldas, which is one of the smallest departments in Colombia. The area is seismically active above the subducting slab of the Nazca plate and deforming upper crust of the Andes and buildings in the region require strengthening against the effects of both types of earthquakes. During these trips, we will discuss the 25 January, 1999, Armenia earthquake (M 6.2) that killed about 2000 people and injured 4000 largely as the result of older, poorly constructed buildings. The economic impact of the quake on the region was significant with about 8000 coffee farms either completely or partially destroyed and over 13,000 structures either partially damaged or completely destroyed.

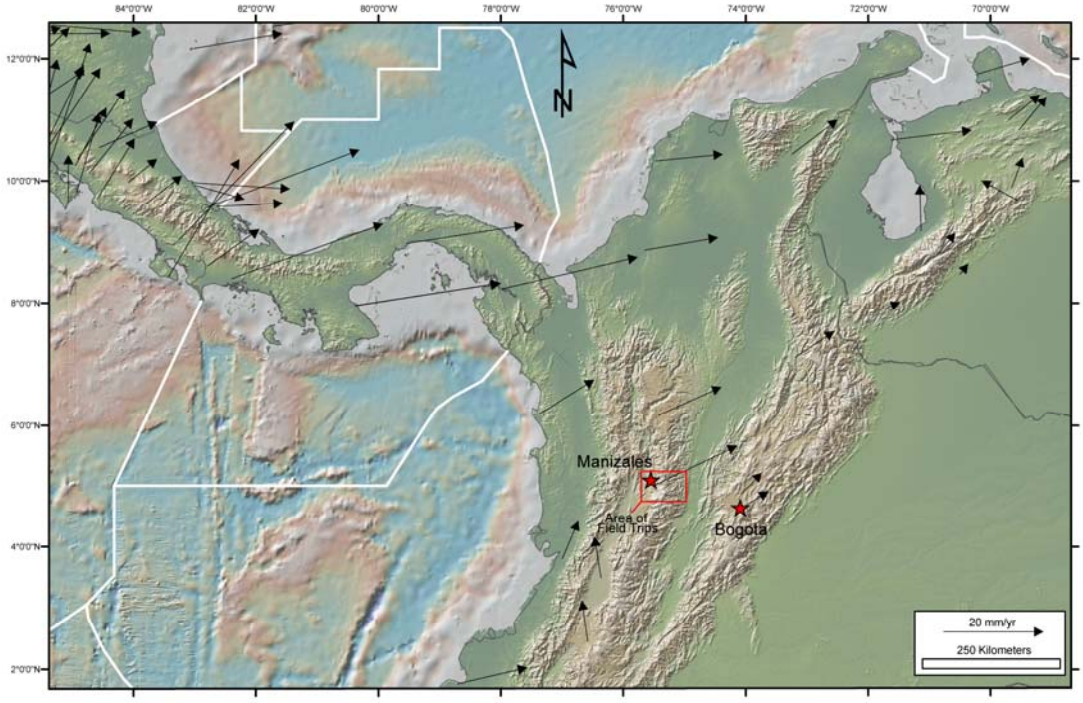

Figure 1 Regional setting of our Penrose field trips in the Manizales area. Black arrows represent GPS vectors with scale in bottom right (Calais et al., 2009). The red box shows the location of a detailed map of the field trip area in figure 2. White lines are offshore maritime boundaries.

The economy of Manizales is largely based on coffee production and processing, the manufacture of steel and car parts, the food industry, and education, including several universities. In the last decade, Manizales has developed facilities for call centers for companies based in Spain.

The regional map in Figure 1 shows the main topographic-bathymetric features of the area that are discussed in greater detail in part 2 of this guide. Figure 2 shows the detailed route of both field trip routes.

Figure 2 Location of field trip stops in the scenic, mountainous terrain we we tour during both field trips.

Both field trips will require your full attention and cooperation to insure that the trip remains on schedule and that you remain safe during these trips. Please be ready in the lobby of the hotel to depart at 7 am on both field trip days; the busses will depart promptly in order to stay on schedule. If you need assistance with waking up that early in the morning please consult with the main desk at the hotel. The hotel will provide food and drinks but you will need to dress properly and bring personal items such as cameras, a small daypack, and a notebook. There is always the possibility of rain showers so please bring appropriate rain gear (e.g., impermeable rain jacket with hood, small umbrella). Temperatures will be cool in the 40s to 60s F so use layers that include a fleece jacket that can be worn beneath your windshell/rain jacket along with hat and gloves. Short walks away from the bus are necessary at some stops and the ground may be wet and slippery - so please wear field boots with ankle support and non-slip soles. The weather may be bright and sunny and since we will be at high elevations, please use sunglasses, sunscreen and a hat to protect yourself from the sun.

For safety, please remain seated at all times while the bus is moving and be careful in placing items in the overhead racks that could fall out when the bus is moving. Many of the field trip stops will be along roads with traffic. Please do not attempt to

cross the road unless told to do so by the field trip leader. When crossing roads, check in both directions for oncoming traffic. Avoid standing in the road with your back to possible oncoming traffic. Please avoid scrambling up steep slopes that could result in your falling or your dislodging loose rocks onto others standing below. If hammering rock samples, use eye protection at all times and be aware of those who may be standing nearby. To keep the trip on schedule, please do not wander away from the leader and group and return promptly to the bus with the group when the field trip leader concludes the stop. The leader will point out the main features of interest at each stop so there is no reason to explore a wider area. Please occupy the same seat on the bus all day long rather than moving seats or changing from bus to bus. This will allow us to make a head count and insure that no one is accidentally left behind. If you notice that someone is missing from your bus after the group returns from a stop, please let the field trip leader and driver know as soon as possible. If you are feel ill, experience motion sickness, altitude sickness, or require a toilet, please let the field trip leader and driver know as soon as possible. If you are uncertain about hiking away from the bus, please feel free to remain on or near the bus. Please give the field trip leader your full attention and avoid talking to others or on cell phones while he or she is addressing the group.

Part 2: Tectonic setting of the field trip areas from sedimentary basins to the upper mantle (Discussion leaders: Carlos A. Vargas and Paul Mann)

The field trip area represents an important break between a steeper dipping slab to the south associated with the active Andean volcanic arc and a shallower dipping slab to the north that is not associated with an active volcanic arc. In the text below, we describe two regional profiles on both sides of this break in the arc and subduction structure based on an attenuation tomographic study of subducted slabs beneath Colombia to depths of 275 km (Fig. 3). Both of these sections are supported by gravity and magnetic models.

Our results indicate a major, ~240-km-long tear in the Nazca slab at latitude 5.4°N that separates a 30-40°-dipping southern area with arc volcanism and a zone of shallow 20-30°-dipping subduction adjacent to the more buoyant Panama arc or "indenter" (Fig. 3, inset map). This east-west slab tear is collinear with the extinct east-west Sandra spreading ridge on the unsubducted Nazca plate which we postulate may have formed the zone of weakness along which the tear formed in the subducted slab (Fig. 3, inset map).

The northern edge of the Panama arc merges without apparent tearing of the Caribbean slab (Fig. 4). The Bucaramanga nest occurs on the downdip continuation of the Panama arc and may reflect ongoing breakoff of oceanic crust from the Panama arc block that has become impeded in the zone of shallow subduction. On this trip, we will examine crustal faults and volcanic products that align along the linear surface trace of the proposed Caldas tear. We will also discuss the earthquake and volcanic hazards associated with this complex, arc-continent tectonic setting that includes the superimposed hazards from both subduction earthquakes and earthquakes produced during shallow crustal deformation.

Tectonic setting of the field trip area

GPS data provides a tectonic framework for understanding the collision of the Panama arc with northern South America (Freymueller et al., 1993; Calais et al., 2009) (Fig. 1; Fig. 3, inset map). Vectors in western Colombia show a marked decrease in velocities consistent with collision near the Panama-Colombia border (Adamek et al., 1988; Duque-Caro, 1990). The east-west direction of vectors shows that east-west shortening is constant over large areas of western Colombia (Corredor, 2003). Vectors on the Maracaibo block of Colombia and Venezuela show a more northward direction consistent with the tectonic escape of the Maracaibo block into the southern Caribbean (Kellogg and Bonini, 1982) (Fig. 3, inset map). Unlike the uniform velocity field in the upper crust known from GPS, the subducted slabs beneath Colombia change dip rapidly from an area of normal oceanic subduction at a dip angle of 30-40° between latitudes 3.0-5.4°N in southern Colombia (Fig. 5) and to an area of shallow subduction with dip angles of 20-30° in the area north of 5.4°N, adjacent to the Panama arc (Fig. 4). The change in dip is abrupt and suggests a right-lateral E–W trending shear zone (hereinafter called the Caldas tear) associated with a slab tear process that can be traced over a distance of ~240 km as shown by the eastward displacement of the zone of intermediate depth seismicity at latitude 5.4°N and beneath the Western, Central and Eastern cordilleras (Fig. 3, inset map).

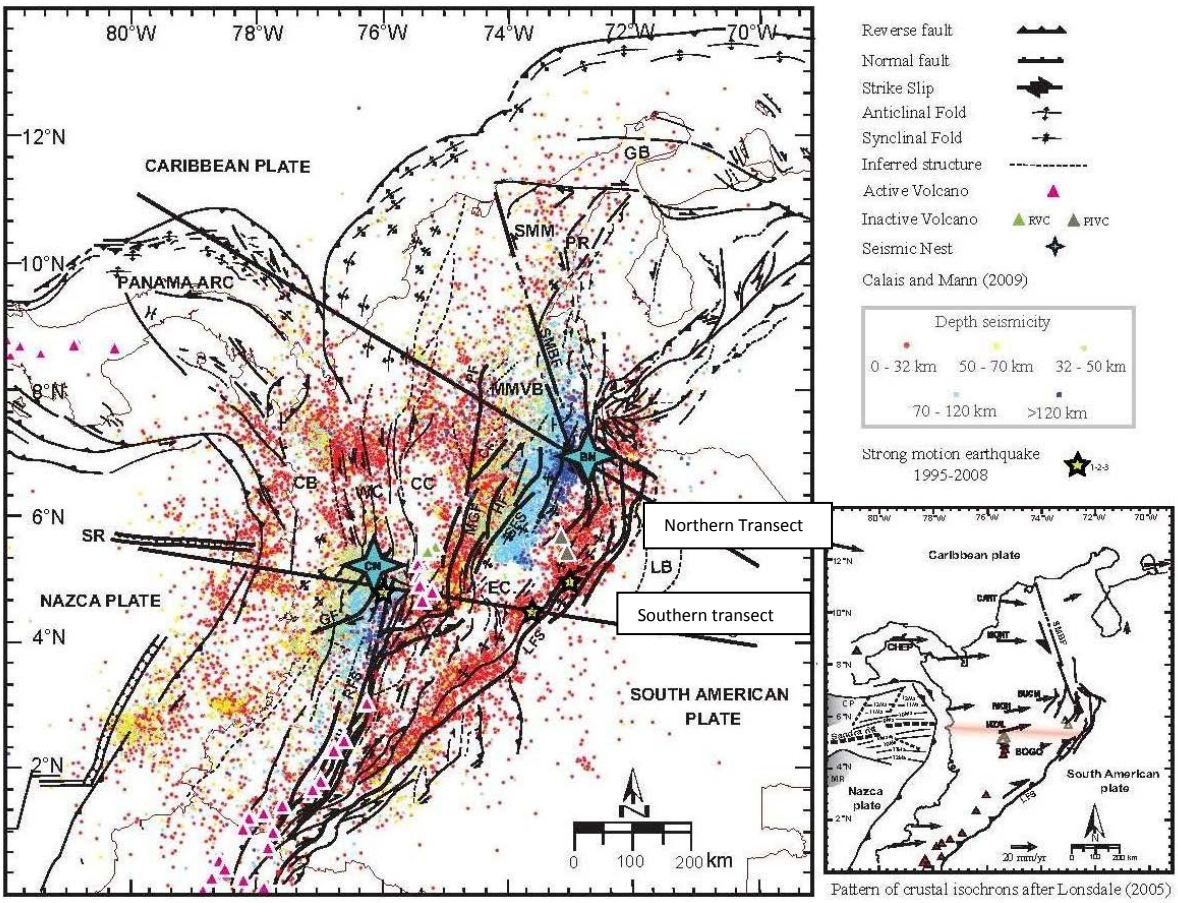

Figure 3. Tectonic setting of Colombia and Panama. Map shows principal plate boundaries, fault systems and neotectonic faults, as well lineaments (dashed lines) and other smaller faults (thin lines). Dots represent hypocentral distribution of the approximately 68,000 earthquakes $1.0 \geq m_L > 6.7$ located by the CNSN between 1993 and 2008. Color scale, continuously varying, indicates the depth of events. Arrows represent station velocity GPS vectors relative to stable South America. CHEP and BOGO denote the GPS's stations used as reference to estimate the onset of the Panama-arc and South American plate collision. Other GPS stations in the Panama-arc collision area are MANZ, RION, BUCM, MONT and CART. The northern and southern profiles are tomographic sections described in this study. Key to abbreviations: SMM, Santa Marta massive; Choco block, CB; Western Cordillera, WC; Central Cordillera, CC; Eastern Cordillera, EC; Perija range, PR; Guajira basin, GB; Llanos foreland basin, LB; Middle Magdalena Valley basin, MMVB; Romeral fault system, RFS; Santa Marta-Bucaramanga fault, SMBF; Palestina fault, PF; Cimitarra fault, CF; Mulato-Getudo fault, MGF; Honda fault, HF; Salinas fault system, SFS; Garrapatas fault, GF; Llanos Fault System, LFS; Ibague fault, IF; Sandra rift, SR; Bucaramanga nest, BN; Cauca nest, CN; Paipa - Iza volcanic complex, PIVC; Ruiz volcanic complex, RVC. Yellow stars correspond to the Tauramena earthquake (Jan. 19th, 1995, M_w=6.5), Armenia earthquake (Jan. 25th, 1999, M_w=6.2) and Quetame earthquake (May 24th, 2008, m_L=5.7).

South of the latitude of the Caldas tear fault, the volcanic chain of the Andean range is active and starts the transition to inactive volcano occurrences with Quaternary ages (Ruiz volcanic complex) (Fig. 3, inset map). The adakitic composition of these volcanoes (Borrero et al., 2009) and the presence of other inactive volcanic bodies to the north of the Caldas tear area, in the Paipa - Iza volcanic complex (Eastern Cordillera), with Pliocene-Pleistocene ages (Pardo et al, 2005) are consistent with melting processes of subducted slabs occurring on both sides of the Caldas tear and perhaps using it as a pathway to the surface (Fig. 3, inset map).

Earthquake tomography has been used in the past for imaging this region (van der Hilst and Mann, 1994; Taboada et al., 2000; Vargas et al., 2007) but differences in their respective resolutions have led to varying proposals for the slab geometry at depth and these interpretations have not been supported by other geophysical data. We present here an integrated study designed to analyze the interaction between the Caribbean and Nazca plates in the northwestern South America and Panama area that is mainly based on the many earthquakes occurring in the region. .

Coda-wave attenuation for imaging plate interactions in northwestern South America

We have used the decay rate of the coda amplitudes (Q_c^{-1}, coda attenuation) of 1674 regional earthquakes located by 17 short-period instruments (*T=1* sec) of the Colombian National Seismological Network - CNSN (Fig. 3). Hypocentral solutions were calculated using the HYPOCENTER (Lienert and Hayskov, 1995) program and the velocity model used by the CNSN (Ojeda and Havskov, 2001). Attenuation estimations were done using the single scattering theory (Aki and Chouet, 1975; Hayskov et al., 1989) in frequency band 1-3 (2 ± 1) Hz and a coda-wave time window of 20 seconds which insures the detection of regional structures. Additionally, a 3D spatial inversion was completed for establishing a deterministic characterization of the spatial heterogeneity in the lithosphere as an alternative technique for traditional tomographic measurements (O'Doherty et al, 1997; Lacruz et al, 2009). Q_c^{-1} is a useful parameter for examining the acoustic contrast between the upper mantle and the lithosphere because seismic attenuation is a physical parameter closely related to the thermal state of the volume sampled by the coda-waves.

Interpretation of the attenuation tomography sections were supported by gravity and magnetic modeling of regional data (Sandwell and Smith, 1997; Maus et al., 2007); geothermal observations were derived from oil wells (Vargas et al, 2009) and geologic transects were compiled with surficial maps and representative seismic lines (Lopez, 2004). The tomographic sections extended from the north (Fig. 4) and south (Fig. 5) of the Panama arc and indenter to as far east as the Llanos foreland basin. These lines cross many interesting tectonic features including: 1) different geomorphological expressions of the northern Andean mountains; 2) the two main earthquake nests of Colombia (Bucaramanga and Cauca); and 3) the main active fault systems of Colombia (Romeral

fault zone, Santa Marta - Bucaramanga fault system, Llanos fault system, Garrapatas fault and Ibague fault).

Flat subduction of the Caribbean plate and coexistence with the Bucaramanga nest: Evidence of a tear propagation process

Tomographic data show the presence of an oceanic crust with thicknesses greater than 20 km related to the Caribbean Plateau (Kerr et al., 1998) with a shallow-subduction angle of <15° over a distance of ~100 km that extends from the South Caribbean deformed belt to the Romeral fault zone (Fig. 4). Beneath Colombia, the dip of the subducted Caribbean slab steepens to 20–30°. Its likely that the interaction of the Caribbean slab with continental crust promotes its subduction at higher angles to intermediate and deep depths (~160 km).

Figure 4. Tomographic section along the northern transect. Coda-wave attenuation anomalies (lower frame) interpreted with overlain gravity and magnetic model (middle frame). Geologic and geothermal observations (upper frame) support the dip changes in the subducted slab.

The seismicity of the Bucaramanga nest is tightly concentrated in the Caribbean slab at depths of 130 to160 km (Zarifi, 2006). There are at least two sets of events forming this pattern and focusing at depths of 80 km and 110 km. Focal mechanisms of the Bucaramanga nest for events reported by NEIC (1977-2009) with $m_b \geq 4.0$ suggest a complex process of fracturing that includes both reverse and strike-slip events. We relate this swarm to a complex tearing process linked to updip shallow subduction of the Panama indenter and the initiation of slab breakoff at depth (Cortes and Angelier, 2005). We have compiled data to show the temporal trend of the swarm using the seismicity

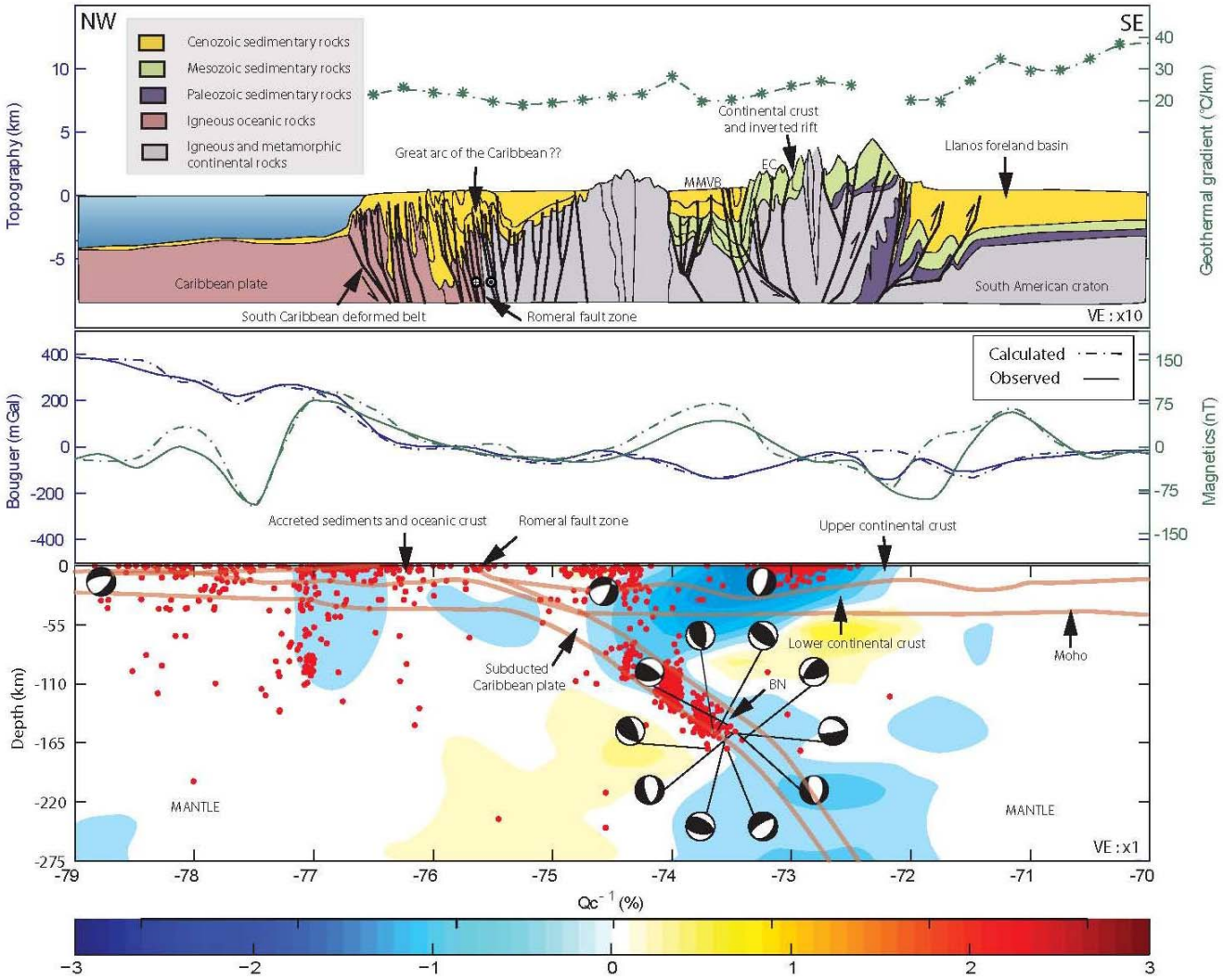

located by the CNSN between 1993 to 2009. A gradual displacement of events northward

and eastward may be due to a tearing in subducting the Caribbean plate, that is slowly propagating to the northeast. The Paipa - Iza volcanic complex dated as 1.9-2.5 Ma (Pardo et al., 2005) is also a possible consequence of the slab tear mechanism, with the nascent tear providing a path for ascending asthenospheric material. Although there is not enough geochemical knowledge to prove that ascending magma is a direct consequence of slab tear processes, the low ratio of Sr^{87}/Sr^{86} (0.705) and the presence of emplaced xenoliths of metamorphic rocks support this interpretation (Jaramillo, 2010).

Normal subduction of the Nazca plate plate and presence of the Cauca nest: Lengthening the Caldas tear?

The tomographically-imaged Nazca slab is 15 to 22 km in thickness and shows a constant subduction angle of 30-40° to a depth >150 km beneath the active volcanic line which are underlain by high attenuation anomalies all consistent with the normal melting range of subducted oceanic crust (Fig. 5). High attenuation anomalies and the presence of shallow to intermediate seismicity around the Romeral fault zone suggest a strong structural control on magmatic activity. A large low-attenuation anomaly corresponds with the low geothermal gradient observations between the Colombia trench and the Central Cordillera and this anomaly may represent volcanic and sedimentary material accreted to the Western Cordillera and Baudo range (Kerr and Tarney, 2005) (Fig. 3). The accretion of this thick sediment package has been proposed to have forced a jump in subduction from along the Romeral fault suture in the Central Cordillera to the present offshore Colombia trench (Cediel et al., 2003).

Two additional attenuation anomalies include: 1) a prominent low anomaly located beneath the Eastern Cordillera and the Middle Magdalena Valley basins and bounded by the Llanos fault system to the east and the Jurassic igneous bodies of the Central Cordillera in the west (Sarmiento-Rojas et al., 2006; Gómez et al., 2005 ; Branquet et al., 2002) ; and 2) a low anomaly beneath the Llanos foreland basin, which has not been previously documented but may represent the continuation of a deeply buried Jurassic rift collinear with the Espino and Apure-Mantecal rifts known in Venezuela (Ostos et al., 2005).

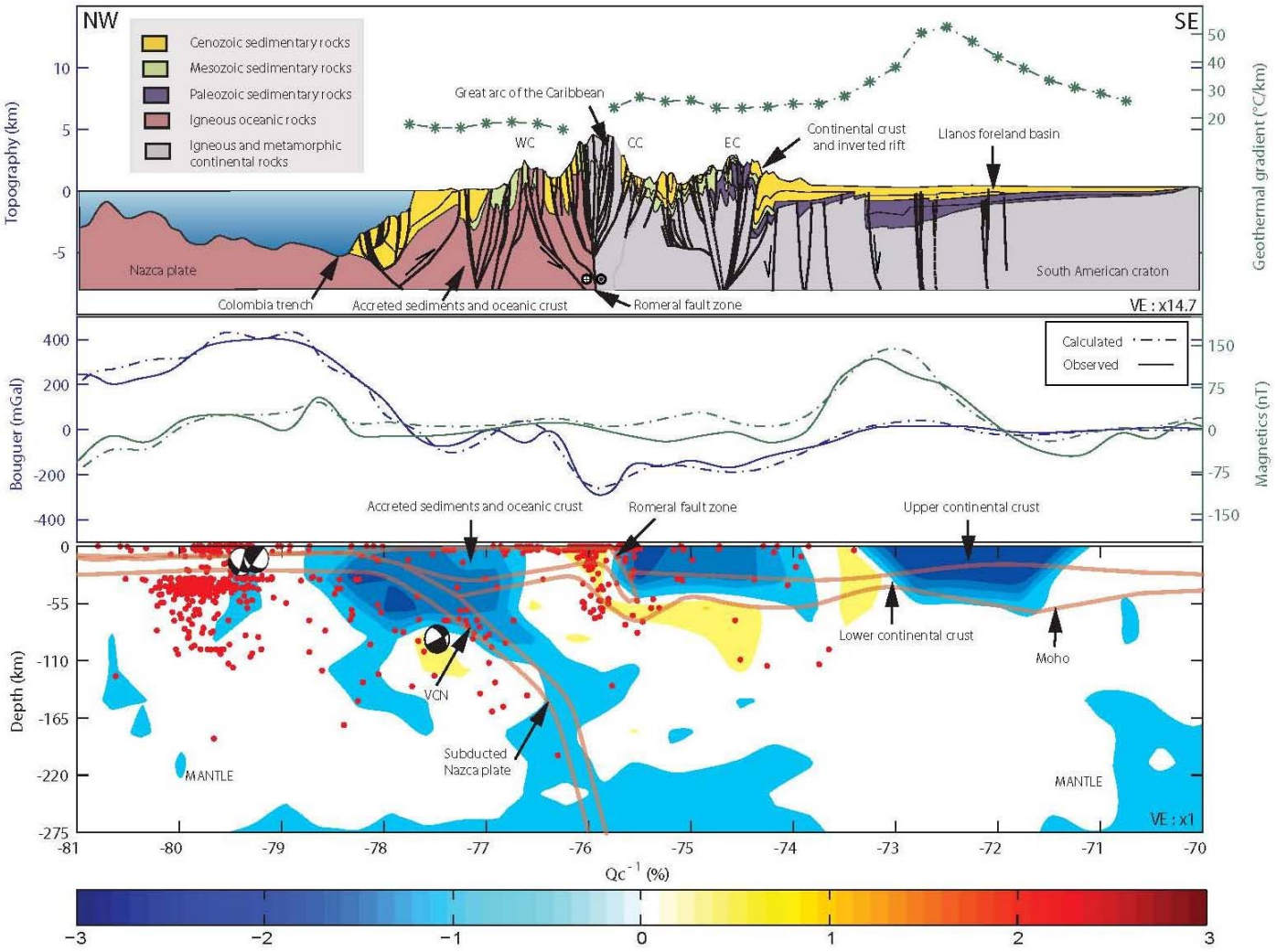

Figure 5. Tomographic section along the southern transect. Coda-wave attenuation anomalies (lower frame), gravity and magnetic model (middle frame) and geologic and geothermal observations (upper frame) showing the subduction geometry of the Nazca plate. Transect crosses the southern part of the Panama arc/indentor and the Cauca earthquake nest.

Seismicity of the Cauca nest is more distributed in depth (70 - 150 km depth range) and its active evolution seems even more complex than the Bucaramanga nest. Its N-S trend is limited to the north by earthquakes with focal mechanisms ranging from pure gravitational collapse in the north to strike-slip events parallel to the Caldas tear fault (Fig. 3). At the southern border of Colombia (latitude 2.5N) there is a shift to a new pattern of intermediate and deep seismicity associated with flat subduction of the broad area of active volcanoes in southern Colombia and northern Ecuador (Gutscher et al., 2000).

Linking the Panama-arc collision with areas of volcanism and seismic nests

Differential displacements between the South American plate and the Panama-arc based on GPS observations suggest a trend of decreasing displacement towards the east (Trenkamp et al., 2002) (e.g. motions at sites of BOGO vs. sites at MZAL, RION, BUCM, MONT and CART). Assuming the BOGO station as a reference point south of the Caldas tear, and the CHEP station as the reference point on the Panama arc-indenter, we estimate ~24 mm/y of effective differential displacement. Given the hypothesis of lateral homogeneity of the crust, constant displacement rate and a seismic offset along Caldas tear of ~240 km, we infer that the onset of the Panama-South America collision began ~10 Ma (Late Miocene). Geologic field observations in the Panama-arc (Coates et al., 2004) suggest that the age for initiation of collision of the Panama-arc against South America occurred between 12.8 to 7.1 Ma, which is consistent with our inferred 10 Ma age for initiation of the Caldas tear. The Sandra rift on the subducting Nazca plate is collinear with the Caldas tear and is thought to have formed the original weakness that would cause the tear in the subducted slab. The age of the Sandra rift is 9-12 Ma (Lonsdale, 2005).

Although there is no evidence of recent activity along the Sandra rift due to lack of instrumentation in the Pacific offshore of Colombia and Panama, recent earthquakes and adakite volcanism along the Caldas tear during last ~4 Ma, are suggesting that this lineament corresponds to a deep-fault-system that allows to move magmatic fluids and generating high geothermal anomalies around it (Vargas et al., 2009). Likewise, the Caldas tear may be responsible of producing large earthquakes along the trend, including the recent strong motion activity associated to the Tauramena earthquake (Jan. 19th, 1995, M_w=6.5). Two types of focal mechanisms have been proposed for this event, one of them suggest an EW-oriented right lateral movement (Dimate et al., 2003) (Figure 2). Similarly seismic activity in the area of the Armenia earthquake (Jan. 25th, 1999, M_w=6.2) shows east-west alignment of aftershocks with the Caldas tear. Moreover, this long right-lateral-weakness-lineament does not seem to work for the Quetame earthquake (May 24th, 2008, m_L=5.7) whose focal mechanism is left-lateral; however the CT may play an important role for controlling the propagation of N-S trending faults (like this event or any related to the Llanos fault system) as has been suggested in the southwest Colombia margin where transverse faults reduce coupling between adjacent segments (Collot et al., 2004).

We removed the crustal earthquakes from the database of events located by the CNSN between 1993 and 2009 in order to illuminate the upper surface of the subducted slabs beneath Colombia (Fig. 6). The 3D model of this surface images the Caldas tear and flat-slab subduction geometry related to the presence of the Panama indenter (Ramos and Folguera, 2009).

A corollary of our model for the Panama indenter and the formation of the Caldas tear is the eastward indentation of geologic features located north of the Caldas tear. Inspection

of the Map of Quaternary faults and folds of Colombia (Paris et al., 2000) suggests that some branches of the Romeral fault system south of the Caldas tear show right-lateral offset from parallel faults including the Palestina, Cimitarra, Mulato-Getudo, Honda or Bituima faults to the north. Other faults with SW-NE trend such as IF and GF could be part of a transfer zone associated with the Caldas tear offset (Fig. 3).

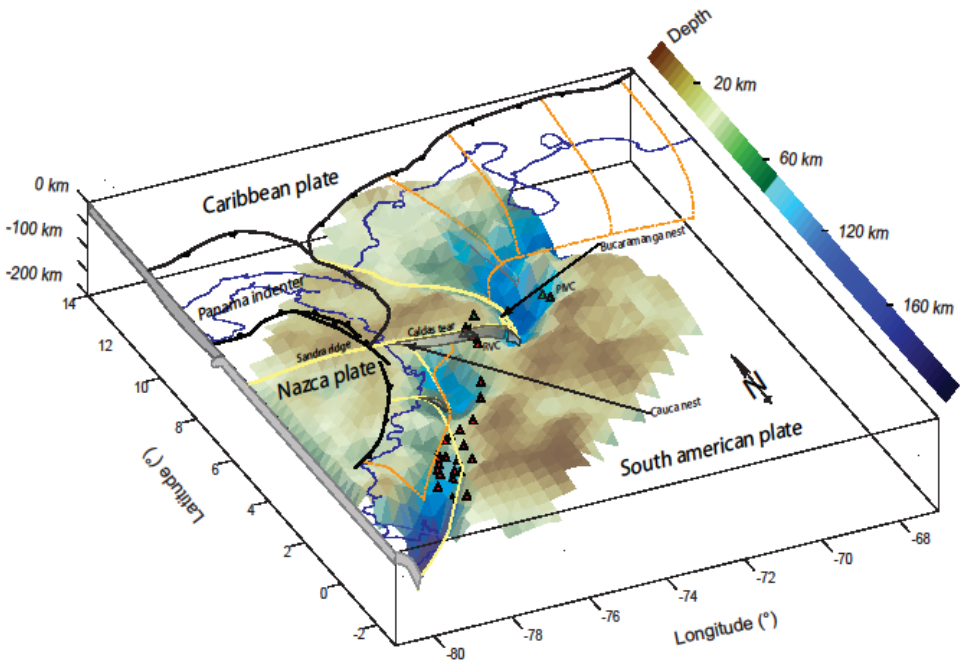

Figure 6. Top surface of subducted slabs beneath northwestern South America estimated from hypocentral distribution of about 68,000 local earthquakes located by the Colombian seismic network (CNSN). A 3D surface was defined by earthquakes and constrains the presence of subducted slabs beneath northwestern South America. Tan lines outline the Panama indentor including the Caldas tear fault to the south. Red triangles show active volcanos formed as a result of slab melting. The Caldas tear forms a major break in the subduction zone and is collinear with the extinct Sandra ridge on the subducting Nazca plate. The Sandra ridge may have acted as a penetrative zone of lithospheric weakness that was reactivated as the Caldas tear fault once the plate was subducted beneath northern South America.

Summary of major points for discussion during this trip:

We combine all observations to propose a regional interpretation of active faults and earthquakes:

1. A buoyant Panama arc acts as an eastward-moving indenter that is ramming into the northern Andes. Indentation produces the distinctive surface fault pattern of V-shaped

strike-slip faults along with widening of the northern Andes by inversion of preexisting Mesozoic foreland basins and widening and deepening of the Llanos foreland basin as a farfield effect (Fig. 3).
2. The indenter point of the Panama arc is aligned with the area of shallowest subduction beneath northwestern South America (Fig. 6).
3. The southern edge of the Panama indenter is sharply defined by the Caldas slab tear along latitude ~5.4°N (Fig. 6). The Caldas slab tear is collinear with the ~9 Ma, extinct, east-west oriented Sandra spreading ridge on the unsubducted Nazca plate which we postulate may have formed the original zone of lithospheric weakness along which the Caldas tear formed in the subducted Nazca slab (Fig. 3, inset map).
4. The northern edge of the Panama arc merges without apparent tearing northward into the Caribbean slab that subducts beneath northwest Colombia (Fig. 6)
5. The Bucaramanga swarm occurs on the downdip continuation of the slab that has preceded the Panama arc into the subduction zone and may reflect and active breakoff of an oceanic slab that has become impeded as it enters the zone of shallow subduction.
6. The surface trace of the Caldas tear corresponds with the occurrence of strong motion earthquakes in the crust including some several, shallow events in past decades.

Part 3: Field guide to the tectonic setting and stratigraphy of the Nevado del Ruiz volcano (Tuesday, January 18, 2011)

Field trip leader: Carlos Borrero, Department of Geological Sciences, Universidad de Caldas, Manizales, Caldas, Colombia (borrero_c@yahoo.com)

Supported by: Maria Luisa Monsalve, INGEOMINAS, Bogota, Colombia (mmonsalve@ingeominas.gov.co)

Carlos A. Vargas, Department of Geosciences, Universidad Nacional de Colombia, Bogota, Colombia (cavargas@unal.edu.co)

Introduction

The subduction of the Nazca oceanic plate beneath the northwestern margin of continental South America is responsible for the generation of Plio-Quaternary line of stratovolcanos and associated belt of magmatism along the Northern Volcanic Zone province of Colombia (NVZ of Bourdon et al., 2003). The Nevado del Ruiz Volcano (NRV) is located in the northernmost end of the NVZ and is part of the previously-named Ruiz-Tolima volcanic complex (Herd, 1982) (Fig. 7).

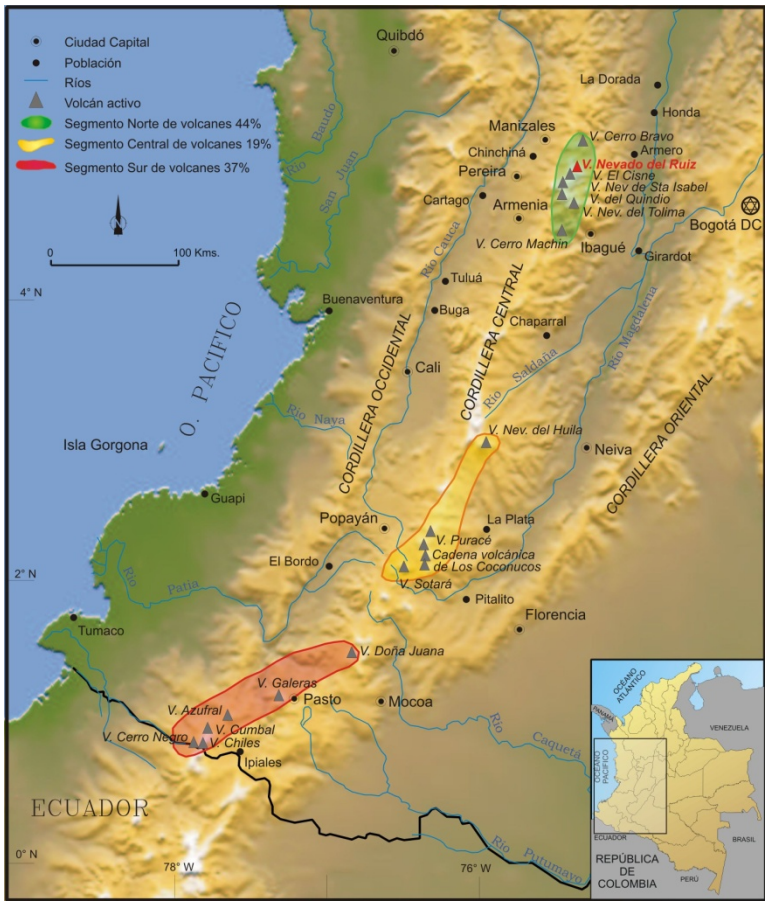

Figure 7. Location map showing the distribution of active volcanic chains in the northernmost part of the Northern Volcanic Zone in Colombia. The green shading highlights the Ruiz – Tolima Volcanic Complex in the Central Cordillera, Colombia, which includes the Nevado del Ruiz volcano (NRV) visited on this trip.

Research on the NRV has been focused on its recent activity including its voluminous November 13, 1985, eruption products along with its associated volcanic hazards. Some authors including Thouret et al. (1990), Vatin-Perignon et al. (1990), and Schaefer (1995), have discussed a stratigraphic model for the NRV using different geomorphic, petrological and geochemical approaches. For the purpose of this fieldtrip, we define the post-1.8 Ma activity of the NRV according to three main stages:

- The **"Ancestral Ruiz"** which includes the stratovolcano construction and a small caldera collapse over the period of 1.8 to 1.0 Ma.
- The **"Older Ruiz"** which includes stratovolcano construction and a small caldera collapse from 0.8 to 0.2 Ma.
- **"Present Ruiz"** which includes composite lava domes during the last 0.15 Ma. The present NRV is composed of andesitic lava flows intercalated with pyroclastic deposits.

Borrero et al. (2009) reinterpreted the former Ancestral Ruiz stage as defined by Thouret et al. (1990) and proposed the hypothesis that the magmatism of the Ancestral Ruiz Volcano must have widened its extent to include several monogenetic vents located around the periphery of the "Present Ruiz". The distribution of these vents was structurally controlled by the Villa María-Termales fault zone located to the south-east of the city of Manizales (González and Jaramillo, 2002). These authors correlate the phases of magmatic activity with the geochemical data and during this trip we will outline a model for the tectonic controls during each of these stages.

During this trip, we will tour this region of spectacular scenery and examine evidence for both the constructional and destructive stages of the Nevado del Ruiz Volcano (NRV). These stages are based on a series of outcrops located mainly along the southeastern and northern edges of the Nevado del Ruiz volcano. During stops 1 to 3 we will examine the main tectonic features that controlled the distribution of the volcanic products during the Ancestral Stage of the NRV.

During stops 4 to 10, we will examine the stratigraphy of the NRV in classic field trip localities that include: 1) the last 11,000 years B.P of tephrostratigraphy related to the main explosive activity of the NRV; 2) different types of pyroclastic, density-current deposits; 3) typical horseshoe-shaped amphitheatres and their associated debris avalanche deposits formed during the Older Ruiz stages; and 4) lava domes and lava flows related to La Piraña stage. We will discuss the subduction and tectonic controls on volcanism in the NRV during all the stops along with seismic and volcanic hazards to the local population.

Tectonic setting of the NRV

The Northern Volcanic Zone (NVZ) of Colombia is defined by a narrow volcanic arc located above the Benioff zone that overlies the steeply subducting slab dipping about 45º to the east (Ojeda and Havskov, 2001) (Fig. 7). The Nazca plate descends below the north Andes at a rate of 56 mm/yr (Trenkamp et al, 2002) (Fig. 1). Information on crustal thicknesses in the region surrounding NRV is limited, but existing gravity data indicate that the crust is 40 to 50 km thick along the topographic axis of the Cordillera Central of Colombia. Despite these data, Schaefer (1995) found evidence for a thin crust (< 35 km) and/or an anomalously dense crust underlying the NRV (Fig. 7).

Nevado del Ruiz Volcano

Nevado del Ruiz Volcano (NRV) is an ice-covered stratovolcano located in the middle Central Cordillera of the Colombian Andes (4º 53'-43'N, 75º 19'-21' W, 5321 meters above sea level), to a distance of 28 km southeast of Manizales, the capital of Caldas department) (Fig. 7). In general, the NRV is a compound volcanic edifice, which encompasses a cluster of lava domes, two small parasitic edifices (La Piraña and La Olleta), and four U-shaped amphitheatres produced by flank collapse and fault activity.

Based on the measured ice thicknesses and interpolated cross-sections, Thouret et al. (2007) estimated the NRV glacial surface area as 25 km^2 before and 21.3km^2 after the 13 November, 1985 eruption of NRV. The ice cap includes seven glaciers, and the ice cap volume was estimated at 0.57± 0.2 km^3 in 2000. By 2003, the Nevado del Ruiz ice cap had lost as much as 52% of its area and roughly 30% of its volume (Thouret et al., 2007).

NRV is one of the northernmost, active volcanoes in the Andean chain of South America. NRV is approximately 150 km above the Benioff zone of the subducting Nazca plate (James and Murcia, 1984) and is one of the northernmost stratovolcanoes of the Ruiz-Tolima volcanic complex (Fig. 7). NRV is part of an arcuate line of nine volcanoes, which form the crest of the Central Cordillera. Hall and Wood (1985) identify this aligned, volcanic group as the northernmost segment in their proposed volcano-tectonic segmentation of the NVZ.

The NRV is intersected by two fault systems: the N20ºE-striking Palestina right-lateral, strike-slip fault system and the N75ºW-striking Villa María-Termales normal fault system (Londoño and Sudo, 2002). Thouret et al. (1990) made detailed studies of the Quaternary eruptive history of NRV and proposed a general stratigraphy formed during three main stages: Ancestral, Older, and Present Ruiz (Fig. 8).

STRATIGRAPHIC MODEL OF NEVADO DEL RUIZ

(AGE DATES FORM THOURET ET AL., 1990, LESCINSKY, 1990, YOUNG, 1991 and SCHAEFER , 1995, AND BORRERO ET AL. (IN PREP.))

PRESENT RUIZ (0.15 Ma - Present)	EVENTS R9 to R0	8630 and B.P. -1985 A.D.
	RECENT AND HISTORICAL TEPHRAS	
	RIO MOLINO PYROCLASTIC FLOWS	3100 and B.P.
	DESTRUCTIVE PHASE (PYROCLASTIC FLOWS)	**10.520-620 and B.P.**
	LAVAS AND DOMES, LOW K SULFIDE	
	LAVAS AND DOMES	
	LA OLLETA PARASTIC DOMES,LAVAS	
	LA PIRAÑA PARSITIC DOME, LAVAS AND PYROCLASTIC	
	CONSTRUCTIVE PHASE (LAVA FLOWS)	O.1 Ma-13.000 and B.P.
OLDER RUIZ (0.8 - 0.2 Ma)	RIO CLARO IGNIMBRITE	0.089 +/- 0.007 Ma
	DESTRUCTIVE PHASE (PF)	
	EL CISNE LAVAS	
	PIRAÑA STAGE	0.24 - 0.15 Ma
	EARLY CONES LAVAS, LOW K SUITE	
	EARLY CONE LAVAS	0.4 +/- 0.1 Ma
	SANTA ISABEL LAVAS	0.76 +/- 0.05 Ma
	CONSTRUCTIVE PHASE (LAVA FLOWS)	**0.76 +/- 0.2 Ma**
ANCESTRAL RUIZ (1.8 - 0.8 Ma)	**DESTRUCTIVE PHASE (PF?)**	**0.97 - 0.77 Ma**
	CONSTRUCTIVE PHASE (LAVA FLOWS AND DOMES)	**1.8 - 0.97 Ma**
PRL PRE-RUIZ LAVAS (1.8 +/- 0.1 Ma)	**VOLCANICLASTIC BASAMENT: DESTRUCTIVE PHASE**	**> 1.5 Ma**

Figure 8. Stratigraphic model of Nevado del Ruiz Volcano modified after Thouret et al. (1990), Lescinsky (1990), Young (1991) and Schaefer (1995). The Piraña stage is proposed by Borrero et al. (in prep.).

Most authors who have studied the NRV all agree that the occurrence of a previous event associated with the Pre- Ruiz Lavas correlates with a destructive phase recorded by volcaniclastic deposits surrounding the NRV area. Lescinsky (1990) and Young (1991) compiled and added new geochronological data especially on recent volcanic events. Schaefer (1995) established a main age for the Rio Claro ignimbrite (formed about 100 ka ago) that defined the limit between the Older and Present Ruiz. Recently, Borrero et al. (in prep.) dated the lavas from the Piraña Cone in order to define the Piraña stage that forms part of the Older Ruiz stage (Fig. 8).

The NRV overlies Paleozoic metamorphic rocks (Cajamarca Complex), Mesozoic sedimentary and volcanic units (Quebradagrande-Alao Complex), and Cretaceous and Paleocene intrusive bodies (Fig. 7). The NRV is located at the intersection of a major right-lateral strike-slip fault (Palestina fault) and a major normal fault (Villa María-Termales fault (Fig. 9). Both intersecting faults have been active throughout the Quaternary (Herd, 1982; Thouret et al., 1990).

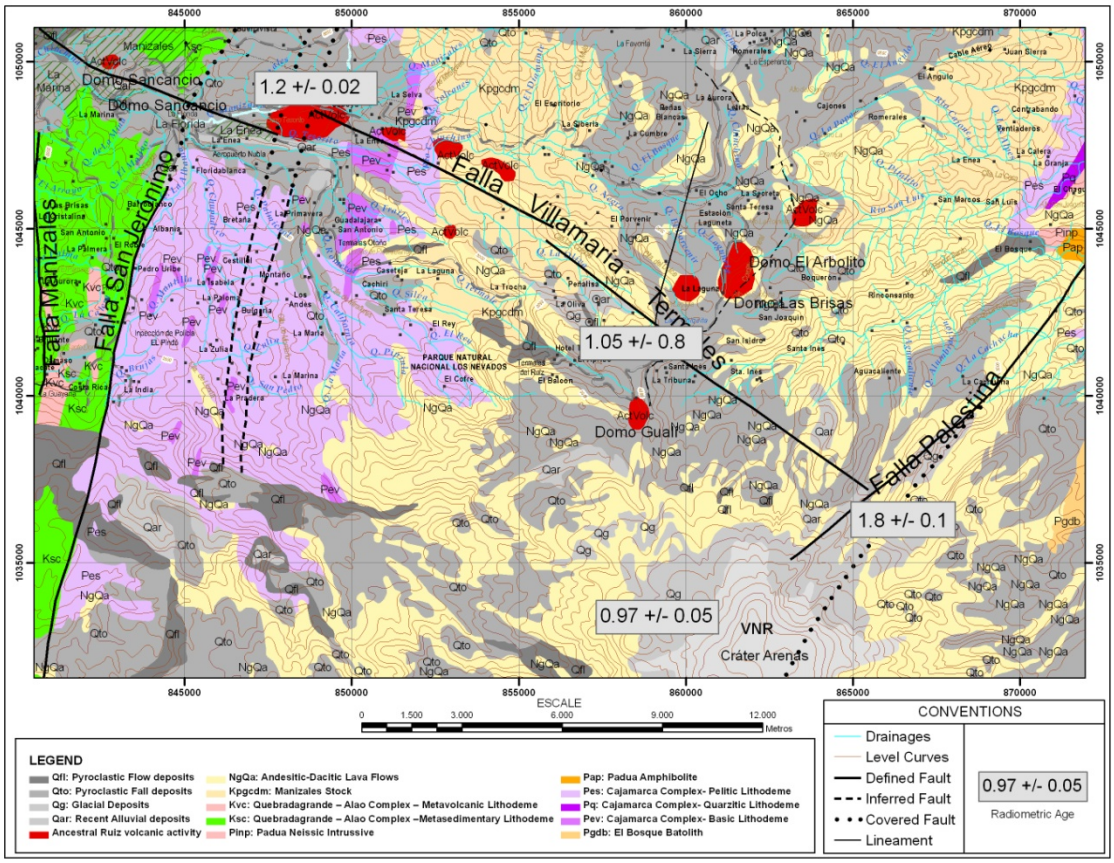

Figure 9. Geological map of the NRV showing its location at the intersection of the Villa María-Termales and Palestina faults. Map modified from Toro et al. (2010) with radiometric ages from Thouret et al. (1990).

Villa María-Termales fault and the NRV

The direct relationships between volcanism and tectonics has remained controversial for many years. The increased recognition of close spatial relationships between faults and volcanic centers as in the case of the NRV has led to construction of models that attempt to explain the observed patterns of regional deformation as well as the distribution, evolution and morphostructure of the volcanic centers. Borrero et al. (2009) suggest that there is a close interaction between tectonics and volcanism in the NRV area, as shown not only by the active faults around the volcano, but also by recent seismicity (Fig. 9).

The Villa María-Termales fault was carefully mapped by González and Jaramillo (2002), based on its straight alignments of numerous geomorphic features including longitudinal valleys, linear depressions, fault scarps, trenches, sag ponds, shutter ridges, saddles, offset features and tilted Quaternary deposits (Fig. 9). These authors also divided the

fault zone into seven fault segments based on variations in physiography and the length of the fault traces as defined by structural barriers composed of north and northeast-striking faults. These fault segments define blocks or wedges each related with relatively higher amounts of seismicity.

Tomographic images of %Vp using first P-arrivals from local earthquakes in the NRV, are used to identify tectonic patterns linked to magmatic activity (Vargas et al., 2000). Figure 10 shows %Vp-tomograms at different depths, that can be used to identify Vp anomalies at northern of the NRV. It is interesting that Vp contrasts at subcrustal depths follow the same trend of the Villa María-Termales fault. This surficial, crustal fault has been proposed by Vargas and Mann (part 2 of this fieldguide) as the surficial expression of the Caldas slab tear, a deep and fundamental fault that separates subducted slabs of different dips (Fig. 3, inset map).

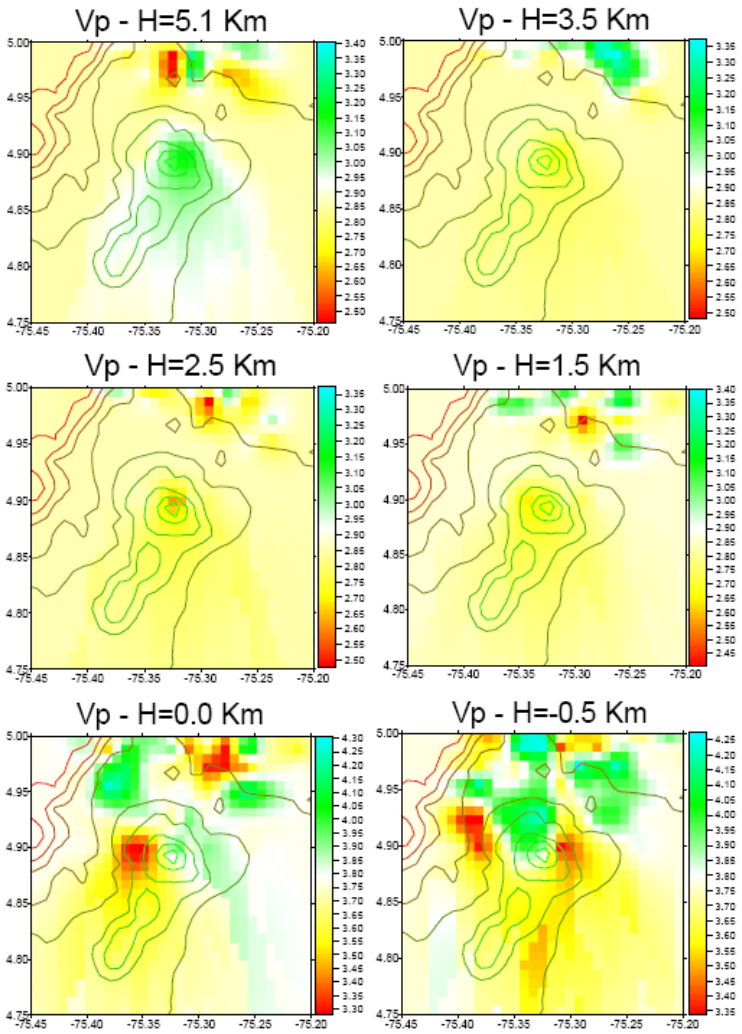

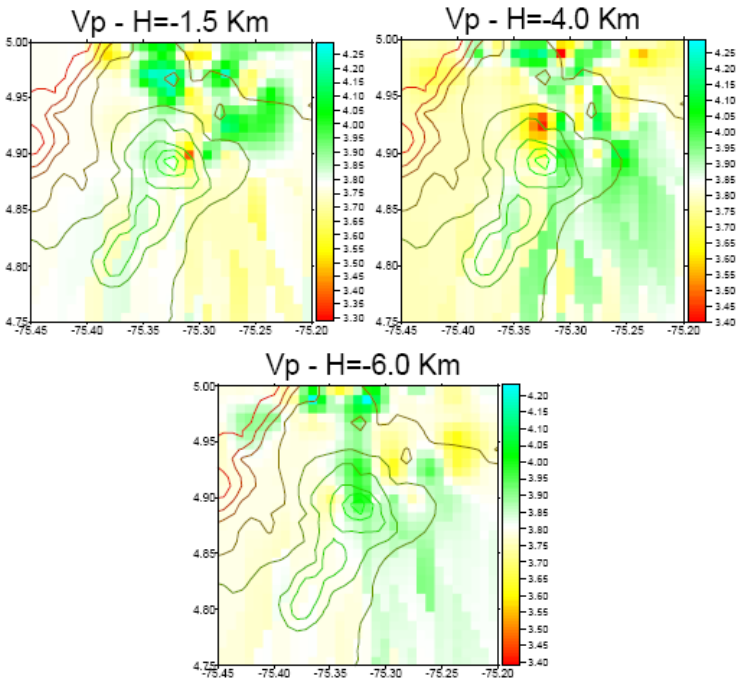

Figure 10. %Vp-tomograms estimates constructed using first P-arrivals from local earthquakes near the NRV (Vargas et al., 2000).

Itinerary of fieldtrip stops on Tuesday, January 18:

Departure: 7:00 am from the Estelar Recinto del Pensamiento Hotel, Manizales (Figure 11). Please assemble in full field gear in the main lobby of the Recinto del Pensamiento Hotel at 6:45 a.m. so we can depart on busses promptly at 7:00 am. Please have your coffee and breakfast before departing, box lunches will be provided by hotel, and we will return to the hotel by dinner time.

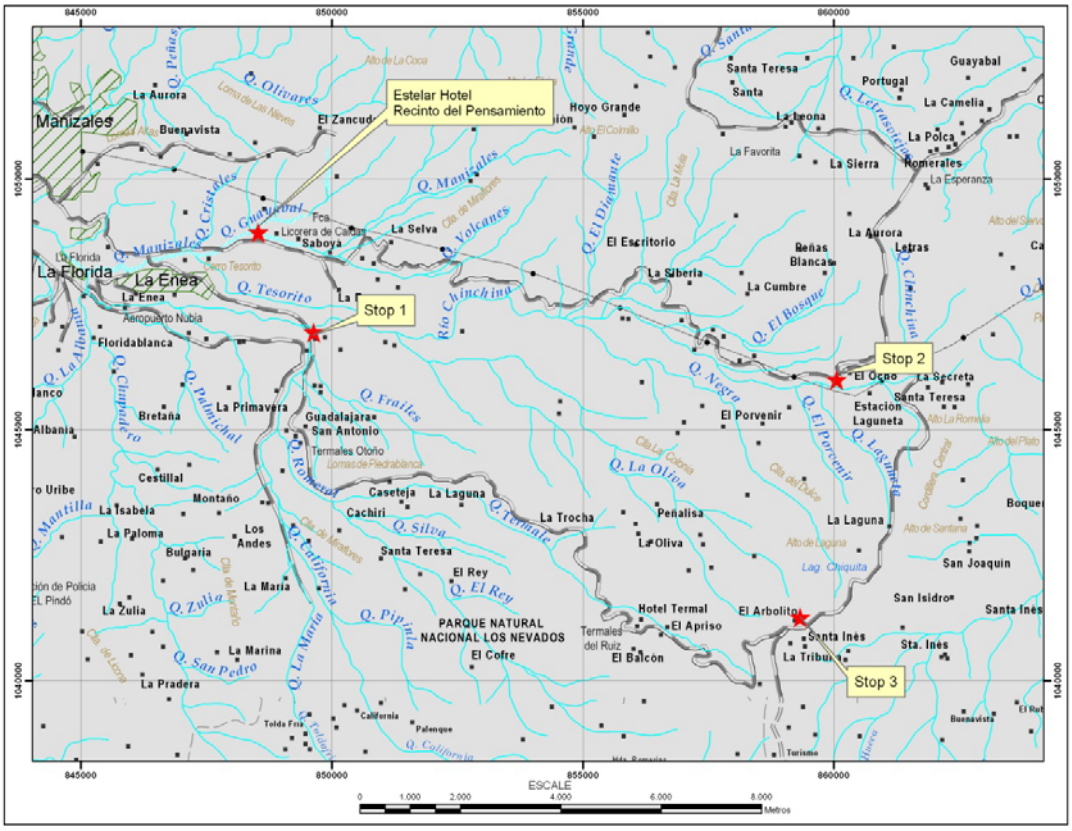

Figure 11. Location of departure site in Manizales and locations of Stops 1 to 3.

Route: Departing Estelar Recinto del Pensamiento Hotel, we will travel east to the La Enea neighborhood for our first stop. From there we will travel west to east on the Manizales-Fresno highway to the La Esperanza rest stop (Fig. 3). While we are in the second stop, we will spend some time to acclimate ourselves to the higher elevations. Please let the leaders know if you feel any intense discomfort. Then we will travel to the south-southeast along the La Esperanza- Brisas dirt road to the third stop, the El Arbolito rest point, and allow some time for altitude acclimatization (Fig. 12). If we are lucky and have clear weather, we will have a wonderful view from here of the Nevado del Ruiz Volcano. From here we will travel to the east on the Brisas-Murillo dirt road visiting the outcrops of the stops 4 to 10 and examine the stratigraphy of the NRV in classic outcrops localities that will include: 1) the last 14.000 yr. B.P tephrostratigraphy related to the main explosive activity; 2) different pyroclastic density current deposits; 3) typical horseshoe-shaped amphitheatres and their associated debris avalanche deposits, and; 4) lava domes and lava flows.

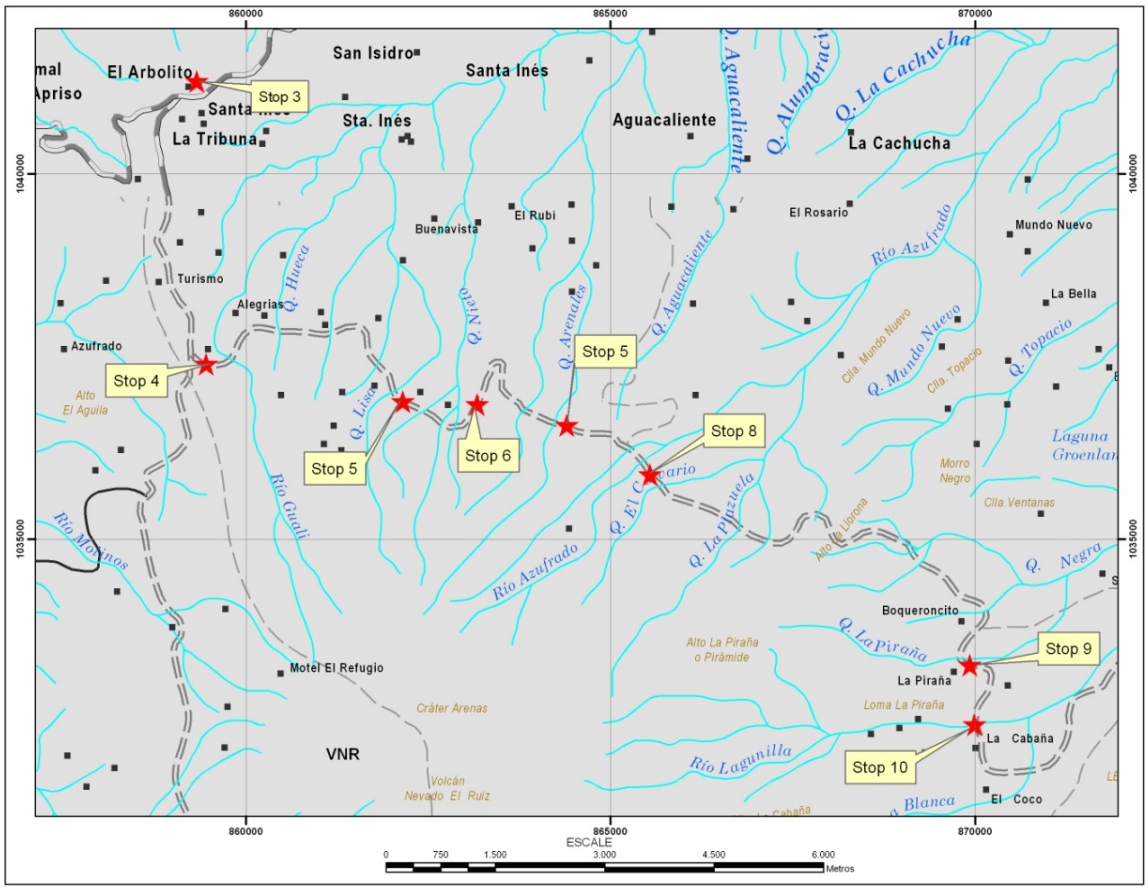

Figure 12. Location Stops 3 to 10, following the dirt road La Esperanza-Murillo.

Stop 1. La Enea neighborhood

A model of the "Ruiz Ancestral" stage (2 to 1 Ma) at the Nevado del Ruiz Volcano was defined by Toro et al. (2010). The extension of the lava remnants of this stage covered an area of about 200 km^2 and were mapped around the northeast-north-northwest sectors of the present edifice of the volcano (Fig. 9). The Ruiz Ancestral Stage was divided in two stages by Borrero et al. (2009), with the first stage corresponding to the Ancestral Lavas and Domes, that define a volcanic cluster aligned with the Villamaría-Termales fault located mainly to the southeast of Manizales in the Gallinazo area (Fig. 13), These domes and flows form a series of aligned hills including Gallinazo, Amazonas, Sabinas, La Oliva and the La Negra domes and lava flows. A second cluster includes lavas located below the Present Nevado del Ruiz area.

At this stop we will examine an alignment of the small "volcanoes" defined by lava domes and lava flows that follow the linear trace of the Villa María – Termales fault zone in the Gallinazo area.

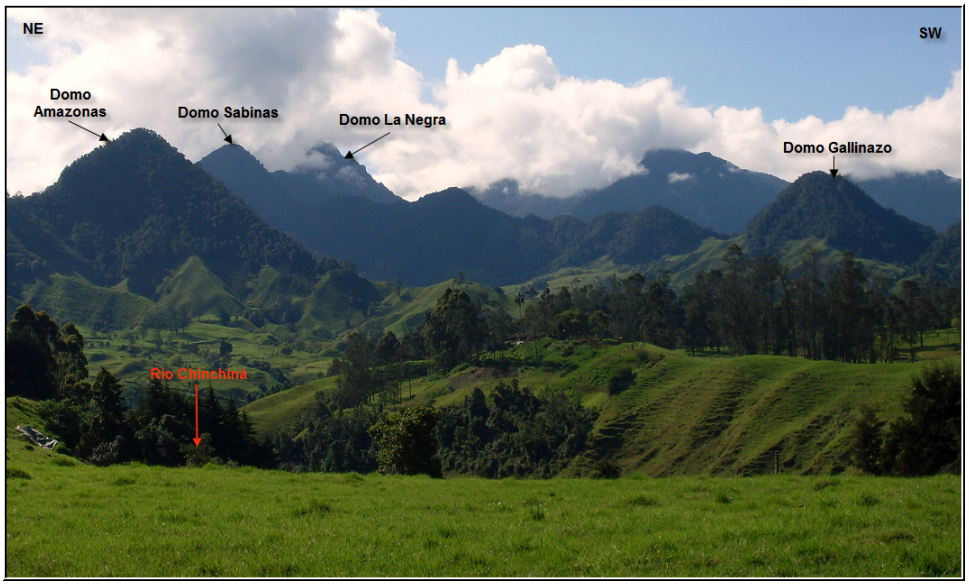

Figure 13. Panoramic view from the ACASA steel recycling plant near Manizales showing alignments of the Amazonas, Sabinas y La Negra, and Gallinazo domes, all of which follow the linear Villa María – Termales fault zone. (Photo credit: Ayala, L.F.).

The volcanic and sub-volcanic rocks of andesitic and dacitic composition in this area are characteristic of adakitic rocks (Toro et al., 2008) (Fig. 14). Both, volcanic and sub-volcanic rocks show high SiO_2 concentrations (63,87-70,15%), Al_2O_3 (14,18-16,83%), low Y (11,20-27 ppm) and Yb concentrations (0,94-1,93 ppm); strong enrichment in Light Rare Earth Elements (LREE) and highly incompatible elements (Rb, Ba), except for Sr which presents low contents and negative anomaly of Nb-Ta, a characteristic that also distinguishes the calcalkaline magmas. Geochemical pattern of LREE and multi-elements show a strong fractionation La/Yb > 8 with typically low contents of Yb ≤ 1.8 ppm , Y ≤ 18 ppm.

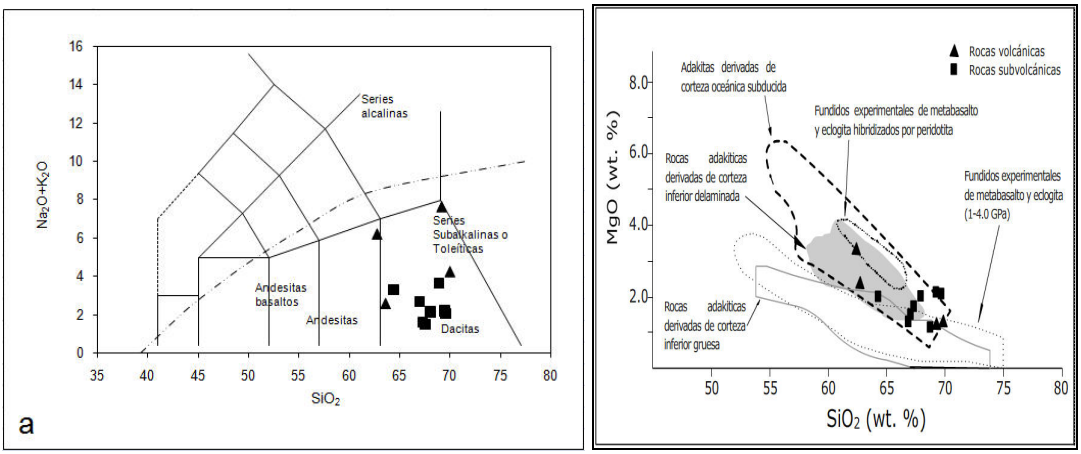

Figure 14. A. TAS diagram. **B.** MgO vs. SiO_2 Harker diagram showing the compositions of volcanic rocks southeast of Manizales (both figures from Toro et al., 2008).

The Ruiz – Tolima volcanic chain in the area of the Ancestral Ruiz stage domes and lavas show adakitic-like signatures. These rocks are located above 110-160 km above the subduction zone using iso-depths from Pedraza et al. (2007) and are about 170 km east of the Colombian oceanic trench where the Nazca plate is subducting eastward beneath the South American continent. The narrow volcanic arc is defined by a single line of active volcanoes. A comparison with the Quaternary Ecuadorian volcanoes that also form part of the Northern Volcanic Zone was made by Toro et al. (2008) who concluded that a flat slab or small-angle slab conditions to 4,5° N latitude during the Late Pliocene-Early Pleistocene could have permitted the formation of the adakite-like rocks.

Additionally, the Post-Ruiz Ancestral volcanic activity does not exhibit typical adakitic signatures (cf. Vatin-Perignon et al., 1990 and Schaefer, 1995), which means a change in the subduction dynamics to this latitude has occurred since 1 Ma. This change probably did not allow continous melting of oceanic crust as is occurring in Ecuador.

Stop 2. La Esperanza

After 30 -35 minutes driving since Stop 1 - and weather permitting – we will have spectacular views of the U-shaped Quebrada Chinchiná, which is an example of a deepened valley glacier on the side of the Ancestral Ruiz edifice. The feature probably represents the glacier stade corresponding to Oxygen Isotope Stage 3, a time when glaciers were still expanding at elevations of 3,000 ± 100 meters above sea level during the LGM (Last Glacial Maximum) ca. 28,000–21,000 yrs B.P. Glaciers shrank considerably from 21000 yr B.P. because of greatly reduced precipitation. This is one of the six Pleistocene cold stades separated by warmer interstades. In this stop, we observe an outcrop of Ancestral Ruiz stage andesite lava flows along the main road (Fig. 15).

Figure 15. Outcrop of Andesite lava flows of Ancestral Ruiz stage.

Whole-rock geochemical data of andesite, dacite and minor basaltic-andesite samples from the different outcrops of the Ancestral Ruiz stage located under and around the present Nevado del Ruiz edifice share calcalkaline affinities with medium to high K contents (Fig. 16). The trace elements range variation compared with SiO_2 suggests a fractional crystallization mechanism. The trace elements pattern is typical of a volcanic arc with Sr, K, Rb, Ba and Th enrichments and Ta-Nb impoverishment. The REE diagram shows a smooth slope with typical LREE enrichment (Toro et al., 2010).

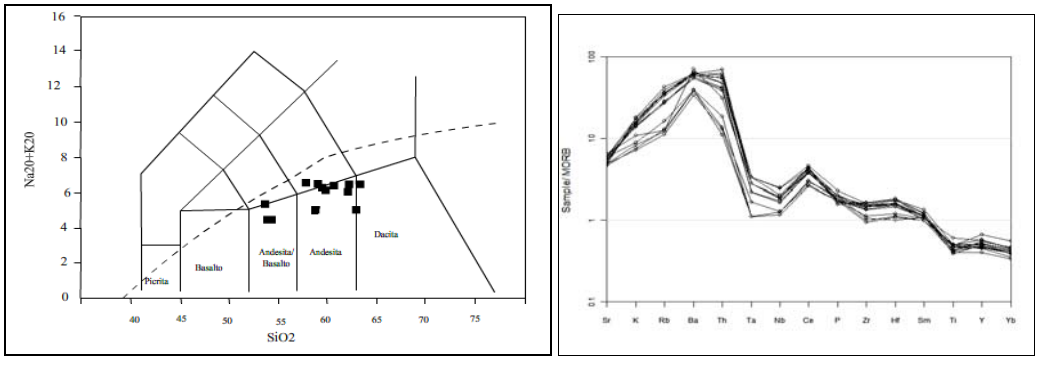

Figure 16. A. TAS diagram **B.** Aracnogram of the Ancestral Ruiz stage volcanic rocks.

Stop 3. El Arbolito (Mirador Cumanday)

This stop located at 3800 meters above sea level is the best viewing point to observe the Present Ruiz edifice composed mainly of lavas and lava domes covered partially by the retreating flat ice cap at the top of the volcano (Figure 17).

Figure 17. Northern face of NRV showing the Gualí- Molinos glacier**.** The boundary between the Older Ruiz edifice and Present Ruiz edifice is located in the area beneath the snow cover. Photo: intranet.ingeominas.gov.co/.../430px-Ruiz03.jpg

From this viewpoint it is possible to observe a striking contrast between the > 60 m thick ice field, forming and blanketing the summit plateau, and the steep northern plateau margin covered by < 30 m of hard ice (ie, the Gualí-Molinos glacier). Aditionally, the equilibrium line altitude (ELA) of this sector is between 5200 and 5100 meters above sea level.

Stop 4. Río Gualí

At this stop we observe some of the main features of the 13 November, 1985, VNR eruption, when lahars initiated at the headwaters of the Gualí River (Fig. 18). Once the avalanches and meltwater floods transformed the debris flows, they remained coherent for up to 104 km in the case of the Gualí River. At this point the debris flow mixed with a relatively larger river system (Río Magdalena).

Figure 18. View of deep Gualí River valley about 3 km downstream from the Arenas crater of NRV showing extensive scour of channel bed with bedrock exposed in many places. Scoured material was incorporated into the lahar. Note small farm buildings for scale.

A brief summary of the events of the 13 November 1985 eruption includes the following events: black ash columns erupted from the volcano at approximately 3:00 pm local time, and were likely produced by a strong phreatic explosion. Between 5:00 and 7:00 pm, the ash stopped falling. The storm's heavy rain and constant thunder in the evening may have overpowered the noise of the volcano, and with no systematic warning efforts, the residents of Armero were completely unaware of the continuing activity at Ruiz. At 9:09 pm, on November 13, 1985, NRV, a small volume of mixed andesite and dacite magma was ejected as pumice fall and pyroclastic density currents during the Plinian eruption that pumped tephra into the atmosphere for more than 30 km (20 mi) - a commercial flight witnessed this eruption. The total mass of the erupted material (including magma) was 35 million metric tons (Naranjo et al., 2006) – only three percent of the amount erupted from Mount St. Helens in 1980 (Krueger et al., 1990). The eruption reached 3 on the Volcanic Explosivity Index. The mass of the ejected sulfur dioxide was about 700,000 metric tons, or about two percent of the mass of the erupted solid material, making the eruption unusually sulfur rich (Krueger et al., 1990).

The 1985 eruption lasted only 20 to 90 minutes but reduced the area of the ice cap by 16% from 25 km^2 to 20.8 km^2 (Thouret, 1990). The corresponding volume of snow and ice loss was estimated to be 6 x 10^7 m^3, or about 9% of the pre-eruption total. An additional 25% of the ice cap area was fractured and/or destabilized (Thouret et al., 2007). The catastrophic lahars triggered by the 13 November, 1985, eruption of the ice-clad NRV demonstrate that the interaction of hot pyroclastic deposits with snow and ice

could release 30–50 million m^3 of meltwater in 30–90 minutes. The 1985 eruption caused a 16% loss in area and a 9% loss in volume of snow, firn and ice. Turbulent pyroclastic density currents mechanically mixed with snow and produced meltwater at a rate of 0.5–1.6mms^{-1} (Thouret et al., 2007). Pyroclastic flows and surges left the ice surface abraded, scoured and gullied on the Nereidas glacier to the west, the Gualí and Azufrado glaciers to the north, the Molinos glacier to the northwest and the Lagunillas glacier to the east.

The complex sequence of pyroclastic flows and surges erupted by Nevado del Ruiz volcano on 13 November, 1985, interacted with snow and ice on the summit ice cap to trigger catastrophic lahars, which killed more than 23,000 people living at or beyond the base of the volcano. The rapid transfer of heat from the hot eruptive products to about 10 km^2 of the snowpack, combined with seismic shaking, produced large volumes of meltwater that flowed downslope, liquefied some of the new volcanic deposits, and generated avalanches of saturated snow, ice and rock debris within minutes of the 21:09 (local time) eruption. About 2×10^7 m^3 of water was discharged into the upper reaches of the Molinos, Nereidas, Gualí, Azufrado and Lagunillas valleys, where rapid entrainment of valley-fill sediment transformed the dilute flows and avalanches to debris flows (Pierson et al., 1990). Computed mean velocities of the lahars at peak flow ranged up to 17 m s^{-1}. Flows were rapid in the steep, narrow upper canyons and slowed with distance away from the volcano as flow depth and channel slope diminished. Computed peak discharges ranged up to 48,000 m^3 s^{-1} and were greatest in reaches 10 to 20 km downstream from the summit. A total of about 9×10^7 m^3 of lahar slurry was transported to depositional areas up to 104 km from the source area. Initial volumes of individual lahars increased up to 4 times with distance away from the summit.

The sedimentology and stratigraphy of the lahar deposits provide compelling evidence that: 1) multiple initial meltwater pulses tended to coalesce into single flood waves; 2) lahars remained fully developed debris flows until they reached confluences with othr major rivers; and 3) debris-flow slurry composition and rheology varied to produce gradationally density-stratified flows (Pierson et al., 1990).

Stop 5. Quebrada La Marcada

During the last 11,000 years, 12 eruptive periods - probably each one with multiple explosive events - have been identified (Herd, 1982). Processes included tephra fallout, pyroclastic density currents, multiple slope failures with debris avalanches and lahars, and interaction with the ice cap (Thouret et al., 1990). In this stop on the upper flanks of NRV outcrops the tephra deposits related mainly with the late Pleistocene - Holocene Plinian to sub-Plinian activity in NRV (~ 11,000 yr. B.P. to present). The outcrop located to the left side of the Quebrada La Marcada shows multi-story deposits of the NRV and Cerro Bravo volcano in their last 3200 yr of explosive activity. In the middle of the outcrop there is a pyroclstic flow deposit (Correa & Penna, 2001, Figure 19) This deposit

called R-5 by Herd (1982) is limited by a 1275 ±50 yr B.P. lower paleosoil and a 1190 ± 120 yr B.P. upper paleosoil (ages from Lescinski, 1990).

In the field, we will discuss various ideas for the origin of this deposit.

Figure 19. Holocene tephra fall with interstratified paleosoils. The middle unit contains a 1275±50 yr B.P. pyroclastic flow deposit (pumice block and ash flow, Correa & Penna, 2001).

Stop 6. La Bodega

In this spot - at the top of the outcrops the ash fall deposits described from Stop 5 - these deposits overlie channelized debris flows and a sequence of layered volcanic deposits. The latter units correspond to diluted pyroclastic density currents (Fig. 20). Taking into account the work of Scolamacchia and Macias (2005), these deposits correspond to a base surge formed during complex eruptions with interaction of magma and external water. The eruptions produced deposits with a radial distribution around the vent with a dispersion of several kms (Sohn, 1996 in Scolamacchia and Macias, 2005). Broad lenticularity and low-angle cross-stratification observed in this outcrop likely will reflect the outward propagation of horizontal density currents from the phreatic eruptive vent. This is an example of how external water could mix with magma in cool environments.

Figure 20. View of the top of the 11,000 yr B.P. ash fall deposits interstratified with paleosols overlying a channelized debris flow and a sequence of wet surges. The age of the surge deposits is unknown.

Stop 7. Río Azufrado – Quebrada La Hedionda

A horseshoe-shaped amphitheater opens out onto the Azufrado River- La Hedionda Creek (Figure 21) (7.5 km long, 2.5 km wide and 1.4 km deep, Thouret et al. 1990). The amphitheatre cut deeply into the Ancestral Ruiz and Older Ruiz edificies in the uppermost north-northeast flank of the Present Ruiz immediately below the rim of the Arenas crater. The glacier tongues, restricted to the amphitheatre, eventually disappeared because they were steep (>35°), thin (<30 m) and were fractured and destabilized during the 13 November, 1985, eruption (Thouret et al., 2007). In addition, these glaciers were covered by thin tephra layers, which decreased the albedo therefore promoting ice melting.

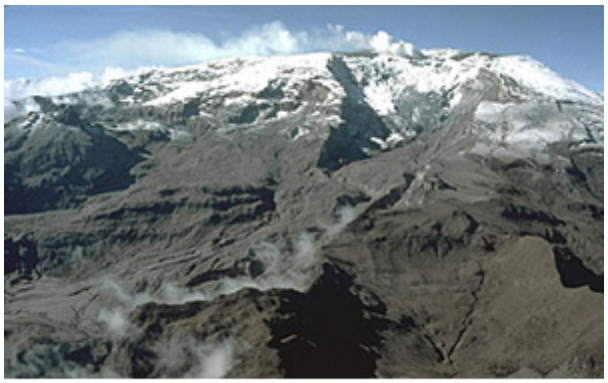

Figure 21. The horseshoe-shaped amphitheatre of Azufrado River produced by collapse of the Northern face of VNR approximately 3100 years B.P. (Thouret et al., 1990). The headwaters is located near the active Arenas crater with the small fumarole. This geomorphic feature resembles the Mt St Helens volcano (US) following its May, 1980, eruption. Photo credit: USGS (Janda, 1985).

López and Williams (1993) suggest that the extent and locations of hydrothermal discharges at NRV may result from the interactions between hydrothermal fluids and the volcanic edifice. Rock dissolution and hydrothermal mineral alteration, combined with physical triggers such as earthquakes, can produce volcanic collapse (Fig. 22). Hot springs and flow paths through the Palestina fault were also contributed to the collapse at the northern face of the NRV. It should be noted that catastrophic volcanic collapse, without precursory magmatic activity, is characteristic of many volcanic disasters.

Figure 22. Close-up of the Quebrada La Hedionda to the right. The valley of this creek was dissected by the >3100 yr. B.P. debris avalanche deposits.

Stop 8. Quebrada La Hedionda

In the stratigraphic section next to the right margin of the Quebrada La Hedionda (Figure 23**),** we can observe from base to top: 1) a lower debris avalanche deposits (at the road level, see the truck for scale); 2) in the middle a sequence of pyroclastic density currents (the layered part of the outcrop); and 3) an upper debris-avalanche deposit.

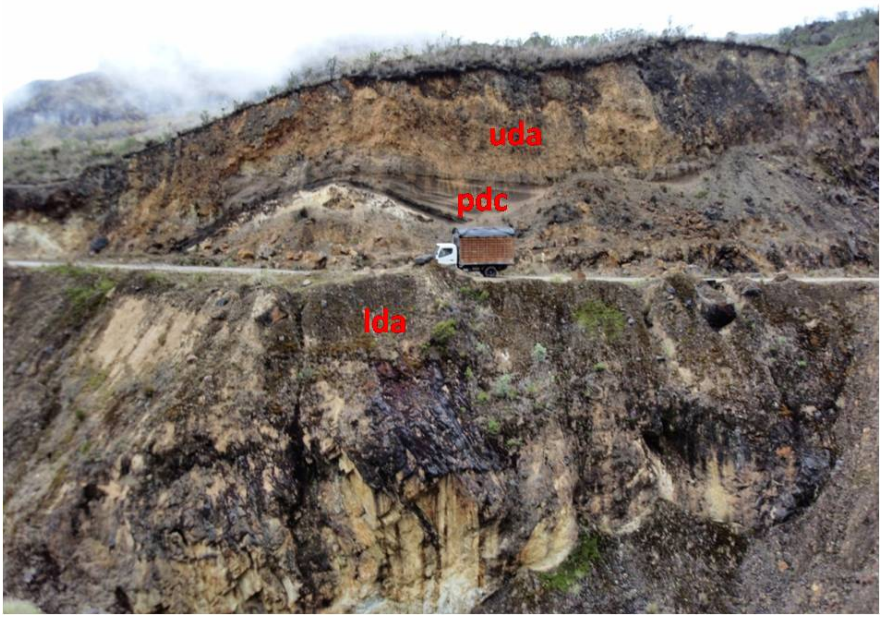

Figure 23. Stratigraphic section of Quebrada La Hedionda, lower debris avalanche deposit (**lda**) that overlies a lava flow of the Older Ruiz edifice, in the middle, pyroclastic density current deposits (**pdc**) and atop, the upper debris avalanche deposit (**uda**).

The lower, thicker debris avalanche deposit shows a hummocky topography and is composed of brightly-colored, hydrothermally-altered, unconsolidated debris. Large blocks up to 10 m across often showing jigsaw cracks, are mixed with a brightly colored, coarse to silty, clay-rich, hydrothermally-altered matrix. This deposit overlies a lava flow (Figure 23) and with no intervening pyroclastic deposit. Thouret et al. 1990 proposed that this deposit belongs to the La Hedionda eruptive stage formed between 3300 and 3100 yr. B.P.

This lower debris avalanche deposit is covered by 1 to 3 m thick sequence of pyroclastic density currents, at the base ash fall deposits composed by medium to fine ash layers interbedded with lithic lapilli and millimeter-size pumice lapilli layers. These tephra are overlain by thin cross-bedded lapilli layers (0.1 to 0.2 m thick) related to a diluted pyroclastic density current. The top unit resembles a dense pyroclastic density current, slightly weathered and with high organic matter content. Thouret et al. (1990) dated a charcoal from this deposit: 3100 ± 70 yr. B.P.

The 10 to 15 m thick upper avalanche deposit conformably overlies the middle sequence of pyroclastic layers. It is similar to the lower debris avalanche deposit, although its surface is less chaotic and hummocky and have a distinctive yellowish-orange hydrothermally altered matrix, and Thouret et al. (1990) proposed a volume of about 0.5 km.

Stop 9. La Piraña area

In this stop we will obverse the La Piraña parasitic cone (Fig. 24), which could be a separate volcano itself, that produce the lava flows that is cut by the road in this point. Recently, Borrero et al. (in prep.) dated these lavas as 146.4 ± 21.0 and 239.5 ± 21.5 ka, and proposed the Piraña stage, a volcanic period framed within the Older Ruiz stage. The whole body of geochemical data is found in Toro et al. (2010)

Figure 24. Panoramic view of the La Piraña parasitic cone, located NNE of the present **NRV** edifice.

Stop 10. Río Lagunillas

In this stop, we visit the Lagunillas valley and at the top the ice cap, the Lagunillas glacier. The glacier is below the horseshoe-shaped scar of rockslide debris avalanche deposits, the trough and glaciated valley, and high lateral moraines of middle Pleniglacial age (> 28,000 yr. B.P.). Additionally, the 15 January, 1995, debris flow deposit is shown by mudlines and splash marks in both sides of the valley.

In the headwaters of the Lagunillas valley, a 2.5 km long, 1 km wide, and 400 m deep horseshoe-shape amphitheater is a conspicuous geomorphic feature related to another sector collapse at the NRV. This feature appears smaller and narrower than the Azufrado river amphitheater and it does not show any obvious tectonic control (Figure 25).

The head-valley scar and hummocky topography in the trough floor suggests that repeated retrogressive landslides have contributed to amphitheatre formation along with glacial erosion. Landslides are favored by hydrothermal alteration of lava flows of the Older Ruiz edifice into the head of the Lagunillas valley.

Figure 25. Lagunillas valley showing the foreground with 15 January, 1995, debris flow deposits. The horseshoe-shaped scar morphology is modified by lateral Pleniglacial age-moraines observed mainly on the left side of the photo.

A recent example of a non-volcanic event is a debris flow of ~550,000 m^3 including ice blocks (Figure 25) that travelled 6 km down the Rio Lagunillas valley on 15 January, 1995 (Guarnizo and Ramírez, 1996). Ice- and rockslides were observed in the head-valley cliffs in April, 1994, but the triggering factor may have been an earthquake as the flow was first reported 15 min after a long tremor. López and Williams (1993) have stressed the role of hydrothermal weathering and fluids in destabilizing volcanic edifices and therefore, the Lagunillas head catchment remains the area most prone to lahar generation because of glacial thickness.

Appendix I corresponds to the Nevado del Ruiz Volcano Official hazard volcanic map. This map will be referred to during the trip.

Field trip leader: Alvaro Nivia, INGEOMINAS, Cali, Valle, Colombia (anivia@ingeominas.gov.co)

Supported by: Fabio Cediel, Department of Geology, Universidad EAFIT, Medellin, Antioquia, Colombia (fcediel@eafit.edu.co)

Andreas Kammer, Department of Geosciences, Universidad Nacional de Colombia, Bogota, Colombia (akammer@unal.edu.co)

Hector Mora, INGEOMINAS, Bogota, Colombia (hmora@ingeominas.gov.co)

Hans Diederix, INGEOMINAS, Bogota, Colombia (hansdiederix@yahoo.es)

Carlos A. Vargas, Department of Geosciences, Universidad Nacional de Colombia,

Bogota, Colombia (cavargas@unal.edu.co)

Introduction

Western Colombia was built by subduction/accretion mechanisms including the addition of oceanic crustal fragments to the continental margin of the northern South American plate (Fig. 1). One accretionary event - produced by the collision of South America with buoyant oceanic plateaus that arrived to the continental margin atop the Farallon Plate - is particularly well documented in the rocks that outcrop to the west of the Cauca-Patia Fault. This fault zone marks the boundary between pre-accretion crustal elements and the Caribbean-Colombian Igneous Province made of Upper Cretaceous oceanic plateau fragments (Kerr et al. 1997, 2002, 2004; Vallejo et al. 2006; Alibon et al. 2008). This plate collision event produced profound deformation both in the pre-accretionary crustal elements and in the portions of the Caribbean-Colombian Igneous Province accreted to the continental margin.

Geologic setting of the field trip area

The highly deformed rocks of the pre-accretionary crustal elements have been mapped by several authors using different approaches (cf. attached map of Cediel, 2010, for the Romeral Suture Zone; Map 1). In order to maintain an official nomenclature, we have included in this field guide a fragment of the last version of the Geologic Map of Colombia (modified from Gómez et al. 2007; Map 2, Figure 26), which separated this

area into three regional belts named, from west to east, the Arquía (NP?-Ma3), Quebradagrande (K1-VCm) and Cajamarca (NP?CA?-Mev) complexes (*sensu* Maya & Gonzalez, 1996).

The Arquia Complex forms a discrete belt that separate the Caribbean-Colombian Igneous Province (ultramaphic, gabbro, basic volcanic [K2-Vm4] and sedimentary (mylonitized) rocks [k2k6-Mds4]) to the west from Lower Cretaceous ultramafic, gabbro (K1-Pm), intermediate and basic volcanic and sedimentary rocks of the Quebradagrande Complex to the east. The Arquia Complex is composed of metamorphic rocks, mainly greenschists and amphibolites and along the belt - located between the Cretaceous belts of mafic rocks - there are also outcrop gneisses (P-Pf, Chinchiná, Manizales) and meta-sedimentary quartzose clastic rocks (Sinifaná Meta-sediments). Both the Arquía schists and the meta-sedimentary rocks are intruded by Triassic undeformed granitoids (Amagá, Cambumbia and Pueblito plutons). In turn, the Lower Cretaceous Quebradagrande Complex is bounded to the east by the Cajamarca complex, composed of metamorphic rocks, including black schists, amphibolites and, gneisses.

Even though the Caribbean-Colombian Igneous Province is separated from the Quebradagrande Complex by the Arquía Complex and despite their differences in age, lithology and geochemical characteristics – Quebradagrande volcanic rocks display supra-subduction zone signature (Nivia et al., 2006). For this reason, these belts were frequently miscorrelated. The correlation problems arise because the geological mapping of the country used the name Romeral fault for all structures that separate metamorphic rocks (either the Cajamarca or Arquia complexes) to the east from sedimentary, basic volcanic, gabbroic and ultramafic rocks located to the west that are included in both belts of oceanic rocks – the Caribbean-Colombian Igneous Province and the Quebradagrande Complex. This interpretation had created a great deal of confusion and so, in order to solve this problem, Maya and Gonzalez (1996) proposed for the structures that separated these belts, a new nomenclature that did not use the term Romeral fault. In this proposal, the Cauca-Almaguer fault marks the boundary between the Caribbean-Colombian Igneous Province and the Arquia Complex; the Silvia-Pijao fault separates the Arquia Complex from the Quebradagrande Complex and the San Jeronimo Fault separates the latter from the metamorphic rocks of the Cajamarca Complex located to the east (Map 2). Some geologists suggest that the Romeral fault name could still be used as the Romeral Fault System to include the three main structural boundaries. It has to be stressed, however, that the boundary between continental and accreted oceanic crust, produced by the collision of the continental plate and the oceanic plateau, corresponds to the Cauca-Patia Fault.

Fieldtrip Itinerary

Departure: We depart 7:00 a.m., Tuesday January 20, from the Estelar Recinto del Pensamiento Hotel, Manizales (Figure 23). Please gather in the front lobby of the

Recinto del Pensamiento Hotel at 6:45 a.m. so we can depart promptly at 7:00 a.m.; breakfast at hotels, box lunches provided, and return by dinner time.

Itinerary: Departing Estelar Recinto del Pensamiento Hotel, we will travel south along the main roadway between Manizales and Medellin, where we will see outcrops of several Cenozoic and Mesozoic units (Fig. 26). The first stop will be in the San Peregrino neighborhood. After 30 minutes of discussion we will travel south on the roadway Manizales-Pereira to the Boqueron stop. We will spend some time observing the landscape and discussing the Abanico del Quindio fan, regional north-south fault trends and Miocene to Recent west-northwest trends. Then we will travel to the northwest to Belalcazar town for a third stop under the Christ sculpture. There we will have discussion about accretion vs. obduction along western of Colombia and have our lunch. After lunch we will travel south to visit stop 4 on the roadway Pereira – Cali and examine the Cenozoic tectonics of the Miravalles syncline. Finally, we will drive to Salento town near to the epicentral area of the Armenia earthquake (January 25, 1999).

Trip preparations: This trip will not involve strenuous hiking, but only short walks away from the bus. Sturdy hiking boots with good ankle support are required. Weather could be cool but might also grow warm (20-30°C). Layered clothing should include a water-proof jacket. Hat, sunglasses, sunscreen and field knapsack are recommended.

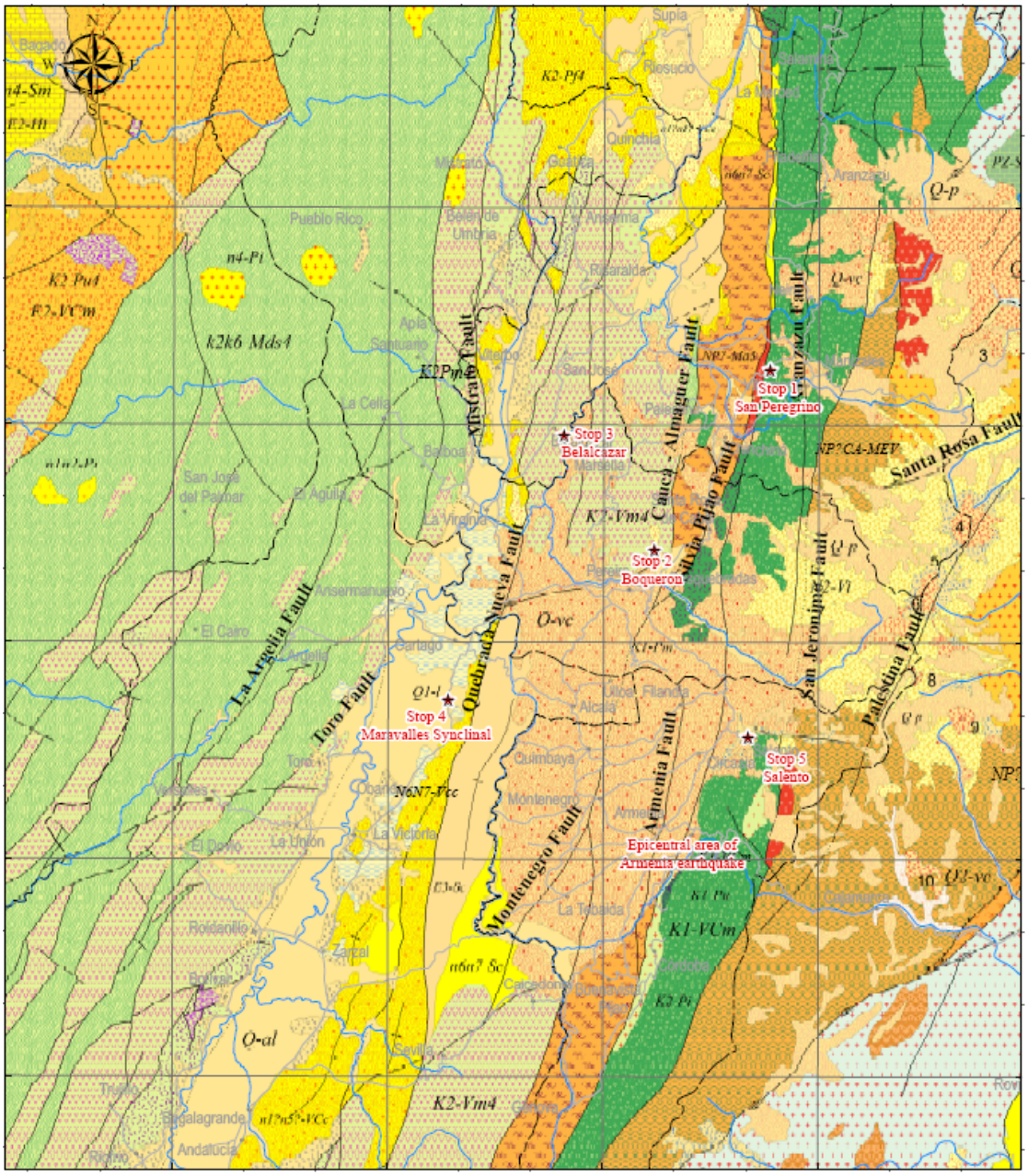

Figure 26. Location of Stops 1 to 5.

Stop 1. San Peregrino

Along the roadway between Manizales to Pereira there are outcrops of the Quebradagrande and Arquia Complexes, as well Neogene units covering the Paleogene, Mesozoic and Paleozoic units. Near to the San Peregrino station it is possible to observe several geomorphologic features associated with the Silvia-Pijao fault. Active tectonics

related to this fault have generated steep slopes that have led to instabilities in the roadway (Figure 27).

During this stop we will discuss about the tectonic evolution of northwestern South America, its regional stratigraphy, as well as differences between the Romeral fault and the Romeral suture zone.

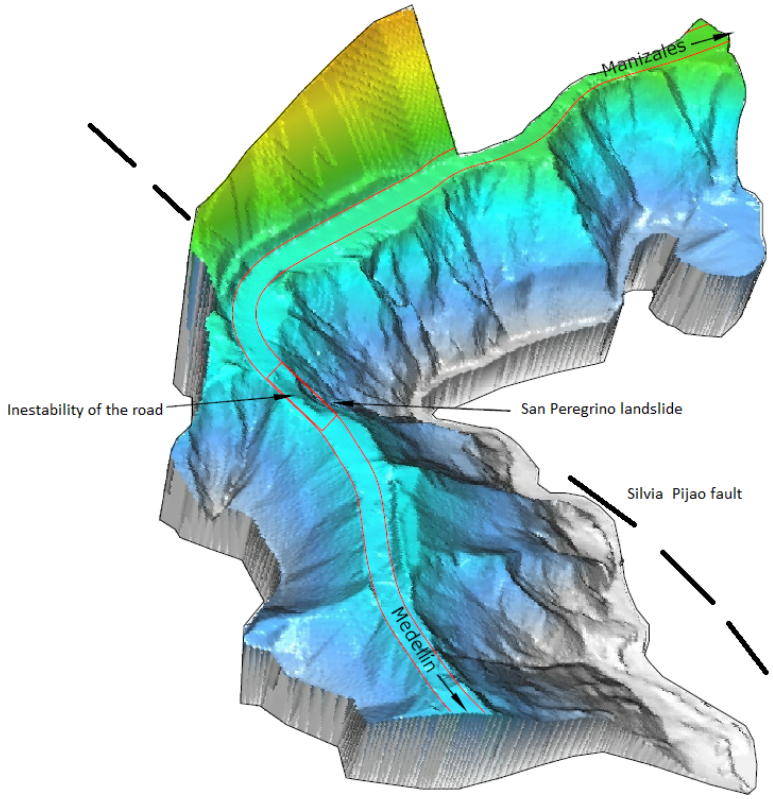

Figure 27. Geomorphologic expression of the Silvia – Pijao fault in San Peregrino. Active tectonics generates instabilities along the roadway connecting Manizales and Medellin. One lane of the road has been damaged and a new bridge was necessary to keep the road open. Modified from Estrada et al. (2009).

Stop 2. Boqueron

This overlook allows us to examine geomorphological features of the Cauca – Almaguer fault, as well the Otun fault of possible Miocene age. Far on the horizon, its possible to see the Quindio fan (Fig. 28), a volcanic-clastic unit that covers several active fault segments of the Silvia – Pijao fault. One segment, the Navarco fault, has been interpreted as a blind fault that produced the Armenia earthquake (M 6.2, Jan. 25, 1999). However, new evidence suggests a more complex fault process was responsible for this event and other seismic activity in the region.

(A)

(B)

Figure 28. Landscape viewed from the Boqueron stop. **A.** The Silvia – Pijao fault and the Otun fault can be observed from this overview. **B.** Steep topographic gradient from Boqueron to Dosquebradas town and Pereira city has been addressed by the construction of this helicoidal bridge-tunnel structure.

Stop 3. Belalcazar

At this stop we will observe larger tectonic structures formed by the accretion of oceanic crust to the western margin of Colombia, as well as evidence for active tectonics along north-south-trending river valleys. This stop shows the geomorphologic expression of accretion associated to the Mesozoic subduction on the western margin of the South American plate (Fig. 29). This accretion has been recognized in Colombia by the presence of Jurassic (Ibague [T3J-Pi]; Mocoa, Algeciras batholiths) and Cretaceous (Antioquia batholith) granitoid rocks that intrude the Cajamarca Complex east of the Central Cordillera. In addition, the Quebradagrande complex has been proposed to belong to the set of rocks formed within intracontinental marginal basins that have been proposed for the Late Jurassic to Early Cretaceous extending from Tierra del Fuego to Mexico through Chile, Peru and Ecuador (Nivia et al. 2006). Åberg et al. (1984) and Aguirre (1987) proposed that these basins might have formed by ensialic expansion or subsidence mechanisms promoted by the roll-back of the subducting lithosphere on this active convergent margin. Rifting led to rupturing of the continental margin leaving metamorphic rocks – Cajamarca and Arquia complexes - on both sides of the basin. Collapse or closure of this basin might coincided with opening of the South Atlantic as has been suggested for the basins in southern Chile (Dalziel, 1981) or might also be due to the collision of the Plateau that sliced and piled up crustal elements of the active continental margin into a highly deformed complex.

Figure 29. Panoramic view from the Belalcazar stop. The building is located on rocks of the Caribbean-Colombian Igneous Province (ultramafic rocks, gabbros, basic volcanic rocks [K2-Vm4]). Far in the horizon appear sequences of oceanic sedimentary mylonitized rocks (k2k6-Mds4) that confirm an accretionary belt parallel to the western coast of Colombia.

It has been proposed that the arrival and accretion of the Caribbean-Colombian Igneous Province to the continental margin choked the subduction zone located along the western end of the Arquia Complex. Choking accommodated the movement of the oceanic plate towards the east and induced a jump of the subduction zone towards the west to the present-day Colombia-Ecuador trench. This trench marks then the western boundary of the accreted materials, including the Choco-Panama Block. The initiation of this new subduction zone had consequences both at depth and in the surface. In the former environment, the new trench gave rise to several pulses of magmatism that has been migrating towards the interior of the continent since the generation of the Santa Cecilia and La Equis volcanic sequences and the Mande Batholith, during the Eocene up to the position of the active to-date Andean volcanoes in the Central Cordillera (N2-Vi, Q-Vi, Q-vc, Q-p). At the same time on the surface, crustal shortening due to the accretion process led to deformation accompanied by crustal thickening and consequent isostatic rebound that favored erosion during the Early Eocene, an episode that can be recognized all over the country by the lack of the corresponding sedimentary record of this age.

Stop 4. Miravalles syncline

This panoramic stop is a good site for discussion of the effects of the isostatic equilibrium between Late Eocene and Early Miocene when a series of forearc basins developed. The subsiding environment of these basins changed from marine to essentially continental (e.g. the Miravalles syncline, Figure 30) with important supplies of volcanic and volcanoclastic components produced by the erosion of products of contemporaneous volcanism. Late Miocene reorientation of deformational stresses - usually ascribed to the readjustment of Pacific oceanic plates that lead to the generation of the Cocos Plate – produced a compressional phase of the Andean Orogen that favored deformation of forearc basins.

Figure 30. Panoramic view of the Miravalles syncline stop along the roadway connecting Pereira and Cali.

Stop 5. Salento and the epicentral area of the Armenia Earthquake

Near Armenia city is Salento town, a small village located at 15 km NNE from the epicentral area of the Armenia earthquake (M6.2, Jan, 25th, 1999, depth=16 km). The panaroma from the Salento stop allows to us to interpret the interaction between N-S and WNW faults formed along the San Jeronimo fault and Caldas tear, respectively.

Figure 31. Panoramic view from overlook near Salento. N-S and WNW lineaments associated with the San Jeronimo fault and the Caldas tear respectively provide evidence for active tectonics affecting the area (ie, triangular facets).

The present-day configuration of the Colombian region - especially in the Andean zone - is related to the interaction of the Cocos, Nazca, Caribbean, South American plates and more recently to the Panama-arc indenter (Late Miocene). This style of tectonics favors the generation of deep earthquakes, but also the occurrence of superficial strong-motion events. In fact, before 1999 earthquake, the regional historic earthquake record in the "Eje Cafetero" region (area of Armenia, Manizales and Pereira) suggested that the Viejo Caldas seismic nest (80-100 km depth with preferential direction N-S) was the main source of the seismic hazard in the area (Figure 31). However, the Armenia earthquake demonstrated that superficial activity of the N-S fault trend (Vargas et al., 2008), associated with blind faults of the Romeral Fault system, or even related to the Caldas tear trend. These fault trends may contribute to the high seismic hazard for cities like Armenia, Manizales, Pereira, Cali, Medellin and Bogota.

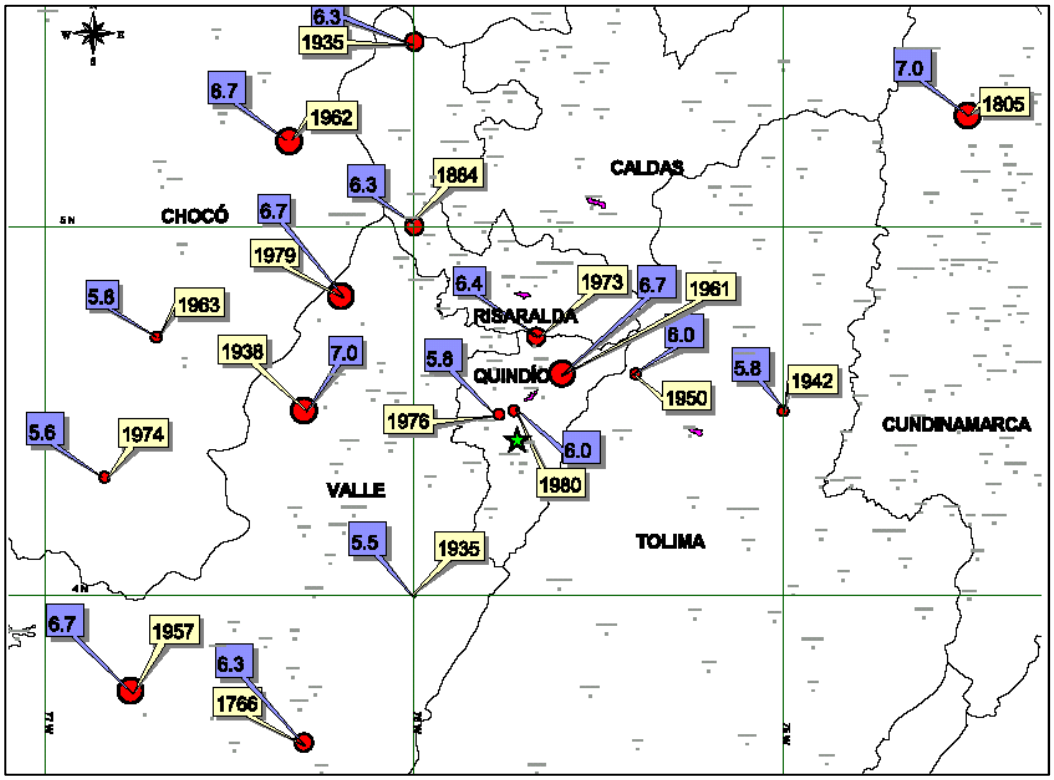

Figure 32. Historical record of strong motion events in the "Eje Cafetero" region. Taken from INGEOMINAS webpage: www.ingeominas.gov.co

References cited

Åberg, G., Aguirre, L., Levi, V. & Nystrom, J. O. 1984. Spreading-subsidence and generation of ensialic marginal basins: an example from the early Cretaceous of central Chile, in Kokelaar, B.P., Howells, M.F. & Roach, R.A. (Eds.), Volcanic Processes in Marginal Basins: Geological Society of London Special Publication 16, 185-193.

Adamek, S., C. Frohlich, and W. D. Pennington, 1988, Seismicity of the Caribbean-Nazca boundary: Constraints on microplate tectonics of the Panama region: Journal of Geophysical Research, v. 93, p. 2053-2075.

Aguirre, L., 1987. Andean modelling: Geology Today, 3, 47-48.

Aki, K., and B. Chouet, 1975, Origin of coda waves: Source, attenuation and scattering effects: Journal of Geophysical Reseach, v. 80, p. 615-631.

Allibon, J., Monjoie, P., Lapierre, H., Jaillard, E., Bussy, F., Bosch, D. and Senebier, F. 2008, The contribution of the young Cretaceous Caribbean Oceanic Plateau to the genesis of late Cretaceous arc magmatism in the Cordillera Occidental of Ecuador. Journal of South America Earth Sciences, 26, 355-368.

Borrero, C., Toro, L.M., Alvarán, M. and Castillo, H., 2009, Geochemistry and tectonic controls of the effusive activity related with the ancestral Nevado del Ruiz volcano, Colombia. Geofísica Internacional, 48: 149-169.

Bourdon, E., Eissen, J.P., Gutscher, M.A., Monzier, M., Hall, M. and Cotton, J., 2003, Magmatic response to early aseismic ridge subduction: the Ecuadorian margin case (South America), Earth and Plan. Sci. Lett., v. 205, 123-138.

Branquet, Y., A. Cheilletz, P. Cobbold, P. Baby, B. Laumonier, and G. Giuliani, 2002, Andean deformation and rift inversion, eastern edge of Cordillera Oriental (Guateque–Medina area), Colombia: Journal of South American Earth Sciences, v. 15, p. 391-407.

Burke, K. , 1988, Tectonic evolution of the Caribbean, Annual Review of Earth & Planetary Sciences, v. 16, 201-230.

Calais, E., and Mann, P., 2009, A combined GPS velocity field for the Caribbean Plate and its margins: American Geophysical Union, Fall Meeting 2009, abstract #G33B-0657.

Cediel, F., Shaw, R. P. & Caceres, C. Tectonic assembly of the Northern Andean Block, in C. Bartolini, R. T. Buffler, and J. Blickwede, eds., The Circum-Gulf of Mexico and the Caribbean: Hydrocarbon habitats, basin formation, and plate tectonics, AAPG Memoir 79, 815– 848 (2003).

Coates, A., L. Collins, M.-P. Aubry, and W. Berggren, 2004, The Geology of the Darien, Panama, and the late Miocene-Pliocene collision of the Panama arc with northwestern South America: Geological Society of America, v. 116, p. 1327-1344.

Collot, J.Y., Marcaillou, B., Sage, F., Michaud, F., Agudelo, W., Charvis, P.,Graindorge, D., Gutscher, M.A. and Spence, G. D., 2004, Are rupture zone limits of great subduction earthquakes controlled by upper plate structures? Evidence from multichannel seismic reflection data acquired across the northern Ecuador– southwest Colombia margin, J. Geophys. Res. **109**, B11103, doi:10.1029/2004JB003060.

Correa, I. and Penna, A, 2001. Evaluación de un depósito de origen piroclástico en el Volcan Nevado del Ruiz datado en 1.275±50 años (in Spanish). Unpublished bachelor's thesis Geology Department Universidad de Caldas. 66 p.

Corredor, F., 2003, Seismic strain rates and distributed continental deformation in the northern Andes and three-dimensional seismotectonics of northwestern South America: Tectonophysics, v. 372, p. 147-166.

Cortes, M., and J. Angelier, 2005, Current states of stress in the northern Andes as indicated by focal mechanisms of earthquakes: Tectonophysics, v. 403, p. 29-58.

Dalziel, I. W. D., 1981. Back-arc extension in the southern Andes: A review and critical reappraisal: Philosophical Transactions of the Royal Society of London, 300, 319-335.

Duque-Caro, H., 1990, The Choco Block in the northwestern corner of South America: Structural, tectonostratigraphic, and paleogeographic implications: Journal of South American Earth Sciences, v. 3, p. 71-84.

Estrada W., Correa, F., Naranjo, J. (2009). El Deslizamiento de San Peregrino. XII Congreso Colombiano de Geología. 7-11 Septiembre de 2009. Paipa – Boyacá, Colombia.

Freymueller, J. T., Kellogg, J. N., Vega, V., 1993, Plate motions in the North Andean region: Journal of Geophysical Research, v. 98, p. 21853-21863.

Gómez, J., Nivia, A., Montes, N.E., Jiménez, D.M., Tejada, M.L., Sepúlveda, M.J., Osorio, J.A., Gaona, T., Diederix, H., Uribe, H. & Mora, M. (compilers). 2007. Mapa Geológico de Colombia. Escala 1:1,000,000. INGEOMINAS, 2 sheets. Bogotá.

González, L. and Jaramillo, C.M. (2002). Estudio neotectónico multi-disciplinario aplicado a la Falla Villa María- Termales. Unpublished Bachelor's thesis. Universidad de Caldas, Manizales, Caldas, Colombia. 298 p.

Gutscher, M. A., Maury, R. C., Eissen, J. P. and Bourdon, E., 2000, Can slab melt be caused by flat slab? Geology, v. 28, 535–538.

Havskov, J, Malone, S., McCloug, D. and Crosson, R.. 1989. Coda Q for the state of Washington. Bull. Seism. Soc. Am. v. 79, 1024-1038.

Herd, D.G. 1982. Glacial and volcanic geology of the Ruiz-Tolima Complex, Cordillera Central, Colombia. Publ. Geol. Especiales INGEOMINAS Bogotá, v. 8: p. 1-48.

INGEOMINAS. 2008. El sismo de Quetame del 24 de mayo de 2008. Aspectos sismológicos y evaluación preliminar de daños. *INGEOMINAS*, Bogotá. Internal report, 90 p. http://seisan.ingeominas.gov.co/RSNC/pdfs/Info_quetame.pdf.

James, D.E. and Murcia, L.A. (1984). Crustal contamination in northern Andean volcanics. J. of the Geol. Soc. of London, v. 141: 823-830.

Jaramillo, J.M. (GMAS Ltd.) 2010. *Personal communication.*

Lescinsky, D.T. 1990. Geology, volcanology and petrology of Cerro Bravo, a young dacitic stratovolcano in West-central Colombia: Unpublished MSc thesis, Lousiana State Univ, 244 p.

Lonsdale, P., 2005, Creation of the Cocos and Nazca plates by fission of the Farallon plate: Tectonophysics, v. 404, p. 28.

Kellogg, J. N., and W. E. Bonini, 1982, Subduction of the Caribbean Plate and basement uplifts in the overriding South American plate: Tectonics, v. 1, p. 251-276.

Kerr, A. C., and J. Tarney, 2005, Tectonic evolution of the Caribbean and northwestern South America. The case for accretion of two Late Cretaceous oceanic plateaus: Geology, v. 33, p. 269-272.

Kerr, A.C. Tarney, J., Kempton, P., Pringle, M. & Nivia A. 2004. Mafic pegmatites intruding oceanic plateau gabbros and ultramafic cumulates from Bolívar, Colombia: Evidence for a 'Wet' Mantle Plume? Journal of Petrology, 45/9, 1877–1906.

Kerr, A.C., Tarney, J., Kempton, P.D., Spadea, P., Nivia, A., Marriner, G.F. and Duncan, R.A. 2002. Pervasive mantle plume head heterogeneity: Evidence from the late Cretaceous Caribbean-Colombian oceanic plateau. Journal of Geophysical Research, 107, B7, 10.1029/2001JB000790.

Kerr, A.C., Marriner, G.F., Tarney, J., Nivia, A., Saunders, A.D., Thirwall, M.M. and Sinton, C. 1997. Cretaceous basaltic terranes in Western Colombia: Elemental, chronological and Sr-Nd isotopic constraints on the petrogenesis. Journal of Petrology, 38/6, 677-702.

Kerr, A. C., J. Tarney, A. Nivia, G. F. Marriner, and A. D. Saunders, 1998, The internal structure of oceanic plateaus: Inferences from obducted Cretaceous terranes in western Colombia and the Caribbean: Tectonophysics, v. 292, p. 173-188.

Krueger, A., Walter, L., Schnetzler, C., and Doiron, S., 1990, "TOMS measurement of the sulfur dioxide emitted during the 1985 Nevado del Ruiz eruptions". J. Volcanol Geotherm Res. 41 (1–4): 7–15.

Lacruz, J., A. Ugalde, C. A. Vargas, and E. Carcole, 2009, Short Note: Coda-Wave Attenuation Imaging of Galeras Volcano, Colombia: Bulletin of the Seismological Society of America, v. 99, p. 3510-3515.

Lienert, B. R. E., and J. Havskov, 1995, A computer program for locating earthquakes both locally and globally: Seismological Research Letters, v. 66, p. 11.

Lopez, C., 2003, Upper crust models of Colombia, Internal Report, INGEOMINAS, Bogota (Colombia), p. 64.

López, D. and Williams, S. 1993. Catastrophic volcanic collapse: Relation to hydrothermal processes: Science v. 260: 1794-1796.

Lowe, Donald R., Williams, Stanley N., Leigh, Henry, Connort, Charles B., Gemmell, J. Bruce, and Stoiber, Richard E. (November 1986). "Lahars initiated by the 13 November 1985 eruption of Nevado del Ruiz, Colombia". Nature 324: 51–53.

Maus, S., T. Sazonova, K. Hemant, J. D. Fairhead, and D. Ravat, 2007, National Geophysical Data Center candidate for the World Digital Magnetic Anomaly Map: Geochemistry Geophysics Geosystems, v. 8, p. Q06017.

Maya, M., Gonzalez, H., 1996. Unidades litodémicas en la Cordillera Central de Colombia. Boletín Geológico INGEOMINAS, **35**, 43–57.

Naranjo, J.L., Siggurdsson, H., Carey, S.N., and Fritz, W. 1986., Eruption of the Nevado del Ruiz volcano, Colombia, on 13 November, 1985: Tephra Fall and Lahars": Science (American Association for the Advancement of Science) 233 (4767): 991–993.

Nivia, A., Marriner, G.F., Kerr, A.C. & Tarney J. 2006. The Quebradagrande Complex: A Lower Cretaceous ensialic marginal basin in the Central Cordillera of the Colombian Andes. Journal of South American Earth Sciences, 21, 423–436.

O'Doherty, K. B., C. J. Bean, and J. Mc Closkey, 1997, Coda wave imaging of the Long Valley caldera using a spatial stacking technique: Geophyscial Research Letters, v. 24, p. 1545-1550.

Ojeda, A. and Havskov, J. (2001). Crustal structure and local seismicity in Colombia. J. of Seismology 5: 575-593.

Ostios, M. Yoris, F., Avé Lallemant, H.G. 2005. Overview of the southeast Caribbean-South American plate boundary zone. GSA Special paper **394**, 53-89.

Paris, G.; Dart, R.L.; Manchette, M.N. Map of Quaternary faults and folds of Colombia and its Offshore regions. USGS. Openfile, Scale 1:2,500,000 (2000). http://pubs.usgs.gov/of/2000/ofr-00-0284/ofr-00-0284.plate.pdf

Pedraza, P., Vargas, C. and Monsalve, H. 2007. Geometric model of the Nazca plate subduction in southwest Colombia . Earth Sci. Res. J., v. 11 no.2: 124-134.

Pierson, T.C., Janda, R., Thouret, J.-C. and Borrero C., 1990, Perturbation and melting of snow and ice by the 13 November 1985 eruption of Nevado del Ruiz, Colombia, and consequent mobilization, flow and deposition of lahars. J. Volcanol Geotherm. Res. 41: 17-66.

Ramos, V.A and Folguera, A. 2009. Andean flat-slab subduction through time. *Geological Society, London, Special Publications*, **327**, 31-54.

Sandwell, D., and W. Smith, 1997, Marine gravity anomaly from Geosat and ERS 1 satellite altimetry: Journal of Geophysical Research, v. 102, p. 10039-10054.

Sarmiento-Rojas, L. F., J. D. Van Wess, and S. Cloetingh, 2006, Mesozoic transtensional basin history of the Eastern Cordillera, Colombian Andes: Inferences from tectonic models: Journal of South American Earth Sciences, v. 21, p. 383-411.

Schaefer, S.J., 1995, Nevado del Ruiz Volcano, Colombia: Magmatic system and evolution, unpublished PhD. dissertation, Arizona State University. 147 p.

Scolamacchia, T. and Macías, J.L. 2005. Distribution and stratigraphy of deposits produced by diluted pyroclastic density currents of the 1982 eruption of El Chichón volcano, Chiapas, Mexico. Rev. Mexicana de Ciencias Geológicas, v. 22, p. 159-180.

Suter, F., M. Sartori, R. Neuwerth, and G. Gorin, 2008, Structural imprints at the front of the Choco-Panama indenter: Tectonophysics, v. 460, p. 134-157.

Taboada, A., Rivera, L. A., Fuenzalida, A., Cisternas, A., Philip, H., Bijwaard, H. and Olaya, J., 2000. Geodynamics of northern Andes: subduction and intra-continental deformation (Colombia), *Tectonics*, **19**, 787-813.

Thouret, J. C., Cantagrel, J. M., Salinas, R. & A. Murcia. 1990. Quaternary eruptive history of Nevado del Ruiz (Colombia). J. Volcanol. Geotherm. Res. 41, 225-251.

Thouret, J.-C., Salinas, R. and Murcia, A. 1990. Eruption and mass-wasting-induced processes during the Late Holocene destructive phase of Nevado del Ruiz volcano. J. Volcanol. Geotherm. Res. 41: 203-224.

Thouret, J.C., Van der Hammen, Salomons, B. and Juvigné, E., 1997, Late Quaternary glacial stades in the Cordillera Central, Colombia, based on glacial geomorphology, tephra–soil stratigraphy, palynology, and radiocarbon dating Journal of Quaternary Science v. 12,, 347-369.

Thouret, J.-C., Ramirez, J., Gilbert-Malengreau, B., Vargas, C A.., Naranjo, J.-L., Vandemeulebrouck, J., Valla, F. and Funk, M. 2007. Volcano–glacier interactions on composite cones and lahar generation: Nevado del Ruiz, Colombia, case study. Annals of Glaciology 45: 115-127.

Toro, L.M., Borrero, C. and Ayala, L.F., 2010, Petrografía y geoquímica de las rocas ancestrales del Volcán Nevado del Ruiz. Boletín de Geología v. 32: 95-105.

Trenkamp, R., Kellog, J.N., Freymueller, J.T. and Mora, H. (2002). Wide-plate margin deformation, southern Central America and northwestern South America, CASA GPS observations, J. of South Am. Earth Sci. 15: 157-171.

Vallejo, C., Spikings, R.A., Luzieux, Winkler, L. W., Chew, D. and Page, L. 2006. The early interaction between the Caribbean Plateau and the NW South American Plate. Terra Nova, 18, 264–269.

Vargas, C.A., Alfaro, C., Briceño, L.A., Alvarado, I. & Quintero, W. 2009. Mapa Geotérmico de Colombia. Proceedings of *X Simposio Bolivariano Exploración Petrolera en Cuencas Subandinas*, Colombia. www.simposiobolivariano.org/WEB2/memorias.

Vargas C.A., Pujades, L., Mora, H., Gil, F., Acevedo, A., Bohorques, O., Patiño, J. and Carvajal, C., 2000. 3D Crustal Structure from Local Earthquake Tomography in Nevado del Ruiz Volcano, Colombia. 95th Annual Meeting Seismological Society of America IGPP/SIO, University of California at San Diego, Seismological Research Letters, 71 (2), 251.

Vargas, C.A., Pujades, L.G. and Montes, l. (2007), Seismic structure of South-Central Andes of Colombia by tomographic inversión. Geofísica Internacional, v. 46 (2), 117-127.

Vargas-Jiménez, C. A., and H. Monsalve-Jaramillo, 2009, 3D Velocity Structure around the Source Area of the Armenia Earthquake: 25 January 1999, Mw=6.2 (Colombia): Boletin de la Sociedad Geologica Mexicana, v. 61, p. 339-351.

Vargas, C.A., Nieto, M., Monsalve, H., Montes, L. and Valdes, M. (2008). The Abanico del Quindio alluvial fan, Armenia, Colombia: Active tectonics and earthquake hazard. Journal of South American Earth Sciences 25, 64–73.

Vatin-Perignon, N., P. Goemans, R. Oliver and E. Parra-Palacio, 1990. Evaluation of magmatic processes for the products of the Nevado del Ruiz Volcano, Colombia from geochemical and petrological data. J. Volcanol. Geotherm. Res. 41, 153-176.

Young, R. H. (1991). Eruption dynamics and petrology of the most recent eruptions of Nevado del Ruiz Colombia, South America, unpublished MSc. Thesis, Louisiana State University, 121 p.

Zarifi, Z., 2006, Unusual subduction zones: Case studies in Colombia and Iran, University of Bergen.